ACR No. L4F06

NATIONAL ADVISORY COMMITTEE FOR AERONAUTICS

WARTIME REPORT

ORIGINALLY ISSUED
June 1944 as
Advance Confidential Report L4F06

COOLING CHARACTERISTICS OF A PRATT & WHITNEY R-2800 ENGINE INSTALLED IN AN NACA SHORT-NOSE HIGH-INLET-VELOCITY COWLING

By Blake W. Corson, Jr., and Charles H. McLellan

Langley Memorial Aeronautical Laboratory
Langley Field, Va.

NACA

WASHINGTON

NACA ACR No. L4F06

NATIONAL ADVISORY COMMITTEE FOR AERONAUTICS

ADVANCE CONFIDENTIAL REPORT

COOLING CHARACTERISTICS OF A PRATT & WHITNEY R-2800 ENGINE INSTALLED IN AN NACA SHORT-NOSE HIGH-INLET-VELOCITY COWLING

By Blake W. Corson, Jr., and Charles H. McLellan

SUMMARY

An investigation has been made of the cooling characteristics of a Pratt & Whitney R-2800 engine as installed in an NACA short-nose high-inlet-velocity cowling (the NACA D_S cowling). The tests were made in the LMAL 16-foot high-speed tunnel of a stub wing and nacelle combination.

The internal aerodynamics of the cowling were studied for ranges of propeller-advance ratio and inlet-velocity ratio obtained by the deflection of the cowling flaps. The engine-cooling tests included variations of engine power, fuel-air ratio, and cooling-air pressure drop.

The engine-cooling data have been presented in the form of the NACA engine-cooling correlation curves, and an illustrative example of the use of these curves for calculation of engine-cooling requirements in flight is included.

INTRODUCTION

The purpose of the present investigation was to establish the cooling characteristics of a Pratt & Whitney R-2800-B engine as installed in an NACA short-nose high-inlet-velocity cowling (the NACA D_S cowling). For the tests the engine was mounted on a stub wing and enclosed by the NACA D_S cowling and a nacelle. This cowling was developed from the NACA C cowling, described in reference 1, to provide a lower-drag installation, higher pressure recovery at the front face of the engine, and a higher critical Mach number. The engine-cooling tests were conducted in the LMAL 16-foot high-speed tunnel.

The engine was operated over a range of power up to rated power. The effects of variation of cooling-air pressure drop and fuel-air ratio upon engine temperatures were measured. The data are presented in a form such that, for a given set of flight and engine-operating conditions, the average and maximum cylinder temperatures may be readily obtained.

DESCRIPTION OF MODEL AND APPARATUS

The model, a full-scale stub wing and nacelle, is shown in figure 1 mounted in the test section of the LMAL 16-foot high-speed tunnel.

The power plant is a Pratt & Whitney R-2800 A-series engine converted to a B-series, which has a normal rating of 1600 horsepower at 2400 rpm. This engine, an 18-cylinder, two-row, radial, air-cooled type, is equipped with a single-stage, two-speed, gear-driven supercharger. The supercharger gear ratios are 7.6:1 for low blower and 9.9:1 for high blower. For this particular engine, only the low blower could be used. The propeller drive, a 2:1 ratio reduction gear, incorporates the standard Pratt & Whitney torque meter, which measures the reaction from the propeller reduction gears. The engine is equipped with a Stromberg PT-13G1 injection-type carburetor.

The propeller is a controllable three-blade Hamilton Standard propeller A6257A-6 with a diameter of 12 feet 7 inches. The cuffs on this propeller had previously been trimmed for a larger spinner than was used in the present tests. The excess clearance between cuff end and spinner surface was therefore reduced by balsa-wood fairings held in place by doped fabric.

The general shape and coordinates of the short-diffuser cowling are given in figures 1 and 2. The cowling exit flaps controlling the engine cooling-air flow extend around the periphery of the cowling except for a short distance at the top where the carburetor duct blocks the exit. The individual exhaust stacks terminate at the cowling exit slot as shown in figure 2. A calibration of the exit area of the cowling, with allowance for these stacks and the carburetor duct, is presented in figure 3.

In addition to the usual engine instruments, provisions were made for measuring the fuel flow, weight flow of engine charge air, cylinder temperatures, weight flow of cooling air, and engine cooling-air pressure drop.

The fuel flow was measured by both a calibrated rotameter and a weigh tank. The weight flow of charge air was measured by a calibrated venturi in an auxiliary charge-air duct. The conventional charge-air scoop was blocked off, and the auxiliary duct brought the engine charge air from out of doors through the venturi, thence through the vertical duct shown in figures 1 and 2 to the carburetor top deck. In this way not only was measurement of the charge air facilitated, but also the danger of engine detonation was minimized because the warm air from the wind-tunnel stream was not used in the engine. Pulsation from the propeller was avoided; and, because the total pressure of both the wind-tunnel stream and the outside air was atmospheric, pressure at the carburetor deck was not sacrificed.

Temperatures were measured by calibrated iron-constantan thermocouples and were recorded on a Leeds & Northrup Speedomax. The cylinder temperatures were measured at the rear spark plug and at the base of all cylinders. The temperatures at the spark plug were measured by gasket-type thermocouples and by a thermocouple embedded in each rear spark-plug boss (fig. 4). The base thermocouples were embedded in the rear of the base flange. The temperature of the engine charge air was measured at the top deck of the carburetor.

The weight flow of the engine cooling air was measured by the four shielded total-pressure rakes and the surface static orifices in the cowling entrance (fig. 5). The pressure tubes for measuring the engine cooling-air pressures were located as shown in figures 6 to 8. Front pressures in the baffle entrance of the front cylinders were measured on only one side because the other baffle entrance was in the wake of a push rod, as shown in figure 7.

The gasoline used throughout the tests met the Army-Navy specifications. This fuel is a blue, leaded gasoline, which has an antiknock rating of 100 octane and a calorific value of not less than 18,700 Btu per pound.

SYMBOLS

p	pressure referenced to free-stream static pressure, pounds per square foot
ρ	mass density of air, slugs per cubic foot
V	velocity, feet per second
q_c	impact pressure, compressible dynamic pressure, pounds per square foot $\left(F_c \frac{\rho V^2}{2}\right)$
F_c	compressibility factor for air $\left(1 + \frac{M^2}{4} + \frac{M^4}{40} + \ldots\right)$
M	Mach number, the ratio of airspeed to acoustic velocity
V/nD	propeller-advance ratio
N	engine rotational speed, rpm
n	propeller rotational speed, rps
D	propeller diameter, feet
α_T	angle of attack of thrust axis, degrees
C_P	power coefficient $\left(\frac{P}{\rho n^3 D^5}\right)$
P	power, foot-pounds per second
V_l	velocity in cowling entrance, feet per second
σ	relative density of air $\left(\frac{\rho}{0.002378}\right)$
σ_a	relative density of air at stagnation point (relative density of cooling air)
Δp	cooling-air pressure drop, pounds per square foot or inches of water
W_a	weight flow of cooling air, pounds per hour or pounds per second
W_e	weight flow of charge air (without fuel), pounds per hour or pounds per second

T_h cylinder-head temperature (average indication of 18 thermocouples embedded near rear spark-plug bosses), °F

T_b cylinder-base temperature (average indication of 18 thermocouples embedded in cylinder-base flanges), °F

T_a cooling-air temperature (stagnation-air temperature in front of engine), °F

T_g mean effective gas temperature, °F

T_{g_b} mean effective gas temperature for the cylinder bases, °F

$T_{g_{80}}$ reference mean effective gas temperature (for 80° F charge-air temperature), °F

T_e charge-air temperature ahead of carburetor, °F

c_p specific heat at constant pressure, Btu per pound per °F (For air, 0.24)

x, y, and z exponents associated with W_a, W_e, and $\sigma_a \Delta p$, respectively

C_1, C_2,...C_6 constants

A coefficient of friction power

B coefficient of blower power

C constant proportional to engine displacement

g acceleration due to gravity (32.2 feet per second per second)

$p_{e_{SL}}$ exhaust back pressure at sea level, absolute, inches of mercury

$p_{e_{alt}}$ exhaust back pressure at altitude, absolute, inches of mercury

AERODYNAMICS OF COOLING-AIR FLOW

The pressure recoveries at the various stations within the cowling were determined for the two extreme positions

of the cowling flaps, gaps of 2.5 and 7.2 inches. These tests were made at 260 miles per hour, with $C_p = 0.20$, $V/nD = 1.9$, and the thrust axis at zero angle of attack.

The pressure recoveries at various stations throughout the cowling are shown in figure 9, expressed as ratios to the compressible dynamic pressure. The plotted values represent the circumferential averages of the readings of the diffuser and individual cylinder pressure tubes shown in figures 5 and 6. The plots of total pressures measured by the cowling-entrance rakes at station A of figure 5 show that, contrary to the expected results, the pressure recoveries are lower for the low-inlet-velocity condition with the cowling flaps closed than for the high-inlet-velocity condition with the flaps open. The propeller blade sections in front of the cowling opening were apparently stalled for the low-inlet-velocity condition because, normally, the higher angles of attack of these propeller sections would result in higher pressure recoveries for the low-inlet-velocity condition.

The front pressures on the front-row cylinders are about the same for the two cowling-flap positions, as shown by curves B of figure 9. The radial distribution of the total pressure over the cylinder is not uniform. The pressure tubes located on the barrel and on the top of the head are out of the blast of air from the diffuser and, consequently, give much lower readings than the tubes on the side of the head, which are well centered in the cooling-air flow. The pressure recovery on the front of the rear cylinders is less than that on the front cylinders and is also more uniform because of the losses of pressure encountered in passing through the space between the front-row cylinders.

The restricted front-cylinder exit passages between the cylinders of the rear row result in higher positive pressures for the flaps closed and in lower negative pressures for the flaps open than were recorded for the rear cylinders. This difference in rear pressures tends to counteract the higher front-cylinder front pressures and to equalize the cooling-air pressure drops across the two rows of cylinders, as shown in the following table:

Location of pressure tubes	Stations	Cooling-air pressure drop (percent q_c) with cowling flaps set	
		2.5 in.	7.2 in.
Front bank			
Top of head	B to C	43	85
Head	B to C	45	98
Barrel	B to C	30	69
Rear bank			
Top of head	D to E	39	95
Head	D to E	37	86
Barrel	D to E	36	82

The pressure drops given for the cowling with the flap open (gap, 7.2 in.) are probably larger than would be obtained in flight because of the greatly increased blocking effect of the extended flaps in the tunnel.

The circumferential pressure distribution for the engine is shown in figures 10 and 11. The front-bank pressures (fig. 10) are fairly uniform with the exception of the pressures for cylinders 2 and 18 and the top head tubes for the flap-open condition. The low pressures on cylinders 2 and 18 are probably due either to bulges in the inner cowling required to clear the distributors or possibly to the breaking down of the flow at this point because of the presence of the blocked-off carburetor-duct entrance just above the top of the cooling-air inlet. The pressure distribution on the rear cylinders (fig. 11) was less uniform for all locations with the cowling flaps closed (gap, 2.5 in.), and with the cowling flaps open the front pressures varied as much as $0.4q_c$.

The results of tests to determine the effects of propeller operation upon the cooling-air pressure drop are shown in figures 12 and 13. The procedure for these tests was to set the cowling-exit flap and to adjust the propeller for constant speed and power; the wind-tunnel airspeed was then varied and pressure measurements were taken through a range of V/nD. This procedure was followed for three cowling-exit-flap settings and for three values of propeller power coefficient. The overall cooling-air pressure drops given in figures 12 and 13

are the reference cooling pressures used in the following section on the cooling characteristics of the average installation. These values were obtained from the tubes shown in figures 12 and 13 by subtracting from the average front-cylinder total-pressure reading the average static reading behind the rear cylinders. Cooling studies for this engine are facilitated because there is no large variation in available pressure drop with either V/nD or the power coefficient C_p.

The relation of weight flow of cooling air to cooling-air pressure drop was determined simultaneously with the pressure-drop tests. The weight flow of cooling air was measured by the entrance total-pressure rakes and static orifices in the diffuser surface. Figure 14 presents the calibration of the total weight flow of cooling air plotted against the pressure drop across the bases and across the heads. Figure 14 is presented to show the order of magnitude of the cooling-air weight flow rather than to define absolute values. The fact that rather widely separated calibration curves are obtained for the various cowling-flap positions may indicate that the baffle-pressure drop was not a satisfactory index for the total weight flow of cooling air as measured by the entrance rakes. As will be shown later in this report, cowling-flap position had no effect on the engine-cooling correlation based on cooling-air pressure drop, and for this reason the cooling-air pressure drop as measured is believed to give a good indication of local cooling-air flow by the cylinders.

ENGINE-COOLING CHARACTERISTICS

The results of the engine-cooling tests are presented in the form of NACA engine-cooling correlation curves (references 2 to 4). This method of correlating engine-cooling data furnishes a means of coordinating engine temperatures with the variables that determine engine cooling. By use of this method relatively few but carefully controlled tests are needed to establish the engine-cooling characteristics. The results of the tests can be reduced by the use of a few simple equations and the correlated data can be presented as two curves. The correlated data can then be used to predict engine temperatures resulting from specified operating conditions or to determine operating conditions required to maintain specified temperature limits.

Résumé of engine-cooling-correlation principles.- The principles of engine-cooling correlation are based on the fundamental laws of heat transfer. The development of a technique for applying these principles has been presented in references 2 to 4. A general statement of the correlation principle is that the ratio of cooling-temperature differential to heating-temperature differential is a function of a relation between internal flow of heating fluid and external flow of cooling fluid. This principle is expressed symbolically by

$$\frac{T_h - T_a}{T_g - T_h} = C_1 \frac{W_e^y}{W_a^x} = C_2 \frac{W_e^y}{(\sigma_a \Delta p)^z} \qquad (1)$$

The NACA method of correlating engine-cooling data is based on the concept that the true gas temperature of the charge and combustion products, which undergoes cyclic variation within the cylinder, may be replaced by a hypothetical mean effective gas temperature T_g. It has been found (reference 4) that, of the several factors which may affect the mean effective gas temperature in engines operating with fixed spark advance, only two vary enough in normal operation to demand consideration. These two factors are the fuel-air ratio and the temperature of the charge before entering the cylinder. A generalization of these effects is expressed by

$$T_g = T_{g_{80}} + \Delta T_g \qquad (2)$$

where ΔT_g is a gas-temperature increment associated with inlet-charge temperature and where $T_{g_{80}}$, the reference mean effective gas temperature, is regarded solely as a function of fuel-air ratio and must be experimentally determined along with the other constants established in engine-cooling-correlation tests.

The precedent (reference 2) of using 80° F as a reference temperature T_e for the carburetor inlet air is followed here. In the absence of a blower the gas-temperature increment is expressed simply by

$$\Delta T_g = 0.8(T_e - 80)$$

The factor 0.8 is empirical but has been found satisfactory.

When a supercharger is employed in the engine induction system, the blower-temperature rise must be included in the gas-temperature increment. Estimation of the blower-temperature rise is based on identification of blower work with heat, which is in turn interpreted as air-temperature rise. The following equation is based on similar analysis given in reference 5:

$$\text{Blower rise} = \frac{(\text{Blower tip speed})^2}{778c_p g}$$

where blower rise is in degrees Fahrenheit, blower tip speed is in feet per second, and 778 is the mechanical equivalent of heat in foot-pounds per Btu. This expression would be inapplicable for calculating intake manifold temperature but is satisfactory for estimating gas-temperature increment in which the effect of fuel evaporation is accounted for by the experimentally determined variation of mean effective gas temperature with fuel-air ratio. The complete expression for gas-temperature increment becomes

$$\Delta T_g = 0.8 \left[T_e - 80 + \frac{(\text{Blower tip speed})^2}{778c_p g} \right] \qquad (3)$$

For the present tests, equation (3) becomes

Low blower

$$\Delta T_g = 0.8 \left[T_e - 80 + 22\left(\frac{N}{1000}\right)^2 \right]$$

High blower

$$\Delta T_g = 0.8 \left[T_e - 80 + 37.5\left(\frac{N}{1000}\right)^2 \right]$$

Correlation procedure.- The values of the exponents x, y, and z in equation (1) are determined from construction curves, which are plots in logarithmic coordinates of the ratio of temperature differentials against the associated variable W_a, W_e, or $\sigma_a \Delta p$. Data for these plots are obtained from tests made in accordance with a test program of which the following is typical:

Type of test	Charge-air flow (lb/hr)	Fuel-air ratio	Cooling-air pressure drop (in. water)	Purpose of test	
Variable pressure drop	7,750	0.08	45	To determine exponents x and z	To establish correlation curve
	7,750	.08	36		
	7,750	.08	29		
	7,750	.08	23		
	7,750	.08	18		
	7,750	.08	15		
	7,750	.08	12		
	7,750	.08	10		
Variable charge air	5,000	0.08	14.2	To determine exponent y	
	6,000	.08	14.2		
	7,000	.08	14.2		
	8,000	.08	14.2		
	9,000	.08	14.2		
Variable fuel-air ratio	4,000	0.055	Adjust for satisfactory cooling	To establish variation of reference mean effective gas temperature with fuel-air ratio	
	4,000	.060			
	4,000	.065			
	8,000	.070			
	8,000	.075			
	8,000	.090			
	12,000	.100			
	12,000	.110			

During the test in which only the cooling-air pressure drop was varied as well as the test in which only the charge-air flow was varied, the fuel-air ratio was held as nearly as possible constant at 0.08. At this value of fuel-air ratio, the datum mean effective gas temperature $T_{g_{80}}$ is established by reference 2 as equal to 1150° F for the heads and 600° F for the bases. The mean effective gas temperature was then computed by use of the following equations, which were derived from equations (2) and (3):

For the heads,

$$T_g = 1150 + 0.8\left[T_e - 80 + 22\left(\frac{N}{1000}\right)^2\right]$$

and, for the bases,

$$T_g = 600 + 0.8\left[T_e - 80 + 22\left(\frac{N}{1000}\right)^2\right]$$

Only low-blower tests were used to establish the correlation and all the quantities pertinent to the correlation were measured after the engine temperatures had become stabilized.

All the engine-cooling correlation test data are presented in tables I to III. A typical construction curve used to obtain the exponent that governs the effect of pressure drop on engine cooling is shown in figure 15. The data for figure 15 were obtained from tests 240 and 241 and are given in tables I and II. Figure 15 is a plot of the ratio of temperature differentials for tests in which the cooling-air pressure drop was varied systematically and the engine charge air was held practically constant at 7750 pounds per hour. Figure 15 is therefore a graph of equation (1) in the following form:

$$\frac{T_h - T_a}{T_g - T_h} = C_3(\sigma_a \Delta p)^{-z}$$

The slope of the curve is -z. From figure 15, $z = 0.321$.

The construction curve used to obtain the exponent that governs the effect of charge-air flow on engine temperature is shown in figure 16. This curve is a plot of the ratio of temperature differentials for tests in which the engine charge air was varied systematically and the cooling-air pressure drop was held practically constant at 14.2 inches of water. Figure 16 is therefore a graph of equation (1) in the following form:

$$\frac{T_h - T_a}{T_g - T_h} = C_4 W_e^{\,y}$$

The slope of the curve is y. From figure 16, $y = 0.565$.

By plotting the ratio of temperature differentials against $W_e^{\,y/z}/\sigma_a \Delta p$, all the data used in fixing the construction curves were plotted on a single curve representing the following form of equation (1):

$$\frac{T_h - T_a}{T_g - T_h} = C_2 \frac{W_e^{\,y}}{\sigma_a \Delta p^z} = C_2 \left(\frac{W_e^{\,y/z}}{\sigma_a \Delta p} \right)^z = 0.560 \left(\frac{W_e^{\,1.76}}{\sigma_a \Delta p} \right)^{0.321}$$

This expression is an engine-cooling correlation equation based on cooling-air pressure drop and is plotted in figure 17. The value of the constant $C_2 = 0.560$ was determined from this graph.

The variation of reference mean effective gas temperature $T_{g_{80}}$ with fuel-air ratio (fig. 18) was determined by tests 242 and 244 (table II) after the correlation line had been established. In this case the charge-air flow and cooling-air pressure drop were measured and their respective exponents were known for each test point. The correlation abscissa $W_e^{\,y/z}/\sigma_a \Delta p$ was computed and the corresponding value of the ratio of temperature differentials (ordinate) was read from the correlation curve of figure 17. The temperatures T_h and T_a were measured. The computation of T_g was then accomplished by

$$T_g = \frac{T_h(1 + \text{Ordinate}) - T_a}{\text{Ordinate}}$$

The reference mean effective gas temperature obtained by use of equations (2) and (3) is

$$T_{g_{80}} = T_g - \Delta T_g$$

This plot of $T_{g_{80}}$ against fuel-air ratio (fig. 18) is essential to general application of the correlation curve.

An engine-cooling correlation based on the weight flow of cooling air is established by a procedure similar to that followed for the correlation based on cooling-air pressure drop. Data from the same tests have been used for both correlations. The construction curve for the correlation based on weight flow of cooling air is presented in figure 19. Curves are shown for cowling flaps open and closed. Figure 19 is a plot of the ratio of temperature differentials for tests in which the cooling-air flow (pressure drop) was varied systematically while the charge-air flow was held practically constant at 7750 pounds per hour; figure 19 is therefore a graph of equation (1) in the following form:

$$\frac{T_h - T_a}{T_g - T_h} = C_5 W_a^{-x}$$

The slope of the curves is -x. From figure 19, x = 0.642.

By plotting the ratio of temperature differentials against $W_a^{x/y}/W_e$ all the data used in fixing the construction curves were plotted on a single curve, for a single cowling-flap position, representing the following form of equation (1):

$$\frac{T_h - T_a}{T_g - T_h} = C_1 \frac{W_e^y}{W_a^x} = C_6\left(\frac{W_a^{x/y}}{W_e}\right)^{-y} = C_6\left(\frac{W_a^{1.14}}{W_e}\right)^{-0.565}$$

This expression is an engine-cooling correlation equation based on the weight flow of cooling air and is plotted in figure 20. Values of the constant determined from figure 20 are: $C_6 = 2.85$ for the cowling flaps closed and $C_6 = 2.61$ for flaps open. The curve of reference mean effective gas temperature (fig. 18), established by means of the correlation based on pressure drop, is also used with the correlation based on weight flow.

Results.- All the graphical matter pertaining to the engine cooling is presented in figures 15 to 31. The preparation and use of figures 15 to 20, which deal with the engine-cooling correlation for the cylinder heads, have been described in the section on correlation procedure. In figure 21 the hottest temperatures indicated by rear spark-plug-gasket thermocouples, as well as hottest head-embedded thermocouples, are compared with the average of all head-embedded-thermocouple temperatures. The data used for plotting figure 21 were obtained simultaneously with the correlation data. As can be seen in figure 21, the relation of hottest to average temperature is dependent on the engine power. The relation is not direct, however, for, at some engine powers in excess of 1100 horsepower, the temperature divergence was less than the maximum indicated by figure 21. It is believed that the hottest temperature indicated by figure 21 for a given average temperature will not be exceeded in practice.

Graphs, similar to those by which the cooling characteristics of the cylinder heads have been presented in figures 15 to 21, are given for the cylinder bases in figures 22 to 28. Data for the bases are given in

table III. Engine speed had no measurable effect on cylinder-head temperatures except through its effect on the blower-temperature rise, which was accounted for. Inasmuch as the heat generated by piston friction has direct effect on the cylinder-base temperatures, the base temperatures are affected by engine speed. The effect of engine speed is shown in figure 25 by the displacement of points from the curve of reference mean effective gas temperature for the bases. Base temperatures at speeds greater than 2120 rpm were greater than indicated by the correlation curve and, consequently, the effective gas temperature was higher; the converse is true for points at low engine speeds.

Typical distributions of cylinder-head and base temperatures for two cowling-exit-flap settings are presented in figure 29. As was found in all tests, the front-cylinder heads ran considerably hotter than the rear-cylinder heads. The difference in the temperature readings was somewhat greater for the embedded thermocouples than for the spark-plug-gasket thermocouples. The temperatures of the front and rear cylinder bases were approximately equal. The variation between front-row temperatures and rear-row temperatures was less systematic on the cylinder bases than on the cylinder heads.

A comparison of the average temperature of the front row of cylinders with the average temperature of the rear row of cylinders is shown in figure 30. Comparisons are made at 800 and 1100 brake horsepower both on the basis of spark-plug-gasket and embedded thermocouples. Figure 30 indicates that the average front-cylinder-head temperature was of the order of 50° F hotter than that of the rear-row cylinder heads at higher powers. Determination of the cause for this temperature difference between front and rear cylinders is beyond the scope of the present paper.

Estimation of charge-air flow.- One of the principal factors involved in a cooling correlation is the internal flow of heating fluid. In internal-combustion engines the flow of heating fluid is most directly related to the charge-air flow. The correlation method, consequently, has been developed with charge-air flow as a primary variable. Inasmuch as charge-air flow is usually not specified for various engine operating conditions, a

method for estimating the charge-air flow required for any condition of engine-airplane operation is necessary in the application of the engine-cooling correlation.

A simple method for obtaining a close approximation to the charge-air flow required for the engine has been developed. This method is based on the assumption that the value of charge-air flow per indicated horsepower at a given value of fuel-air ratio is unique. A single curve (fig. 31) showing variation of the ratio of charge-air flow to indicated horsepower with fuel-air ratio is used in conjunction with an expression of the following type:

$$ihp = bhp + \left[A + B\left(\frac{W_e}{1000}\right)\right]\left(\frac{N}{1000}\right)^2 - C\left(p_{e_{SL}} - p_{e_{alt}}\right)\left(\frac{N}{1000}\right) \qquad (4)$$

where

ihp indicated horsepower as defined by equation (4)

A coefficient of friction power

B coefficient of blower power

C constant proportional to engine displacement

The coefficient of friction power A in the expression for indicated horsepower has been computed on the basis that the engine friction, without charge air and blower, absorbs 155 horsepower at 2400 rpm. This usage assumes that all the friction is laminar fluid friction within the oil film between moving parts and that the power therefore varies as the square of the engine speed. For this engine, therefore,

$$A = \frac{155}{(2.4)^2} = 27$$

The coefficient of blower power B was calculated by assuming a blower-drive efficiency of 87 percent for the blower and by equating blower power to the rate of energy input to the charge air (reference 5), as follows:

$$\text{Blower hp} = \frac{1}{0.87 \times 550}\left[\frac{\pi N(\text{Impeller diam.})(\text{Blower gear ratio})}{60}\right]^2\left(\frac{W_a}{3600g}\right)$$

$$B = 0.0495\left[(\text{Impeller diam.})(\text{Blower gear ratio})\right]^2$$
$$= 0.0495(0.917 \times 7.6)^2$$
$$= 2.4$$

The constant C provides for the power increase with altitude due to the decrease in exhaust back pressure. By allowing a pressure of 70.7 pounds per square foot per inch of mercury, the power increase is

$$hp = \frac{70.7 \times \text{Engine displacement}}{2 \times 1728 \times 60 \times 550}\left(p_{e_{SL}} - p_{e_{alt}}\right)^N$$

$$C = 0.00062(\text{Engine displacement})$$
$$= 1.735$$

where the engine displacement is measured in cubic inches.

The expression of indicated horsepower then becomes

Low blower

$$ihp = bhp + \left[27 + 2.4\left(\frac{W_e}{1000}\right)\right]\left(\frac{N}{1000}\right)^2 - 1.735\left(p_{e_{SL}} - p_{e_{alt}}\right)\left(\frac{N}{1000}\right) \quad (5)$$

High blower

$$ihp = bhp + \left[27 + 4.05\left(\frac{W_e}{1000}\right)\right]\left(\frac{N}{1000}\right)^2 - 1.735\left(p_{e_{SL}} - p_{e_{alt}}\right)\left(\frac{N}{1000}\right) \quad (6)$$

The constants given in equations (5) and (6) are not intended to be used individually for the calculation either of friction and blower horsepower or of the power obtained from decreased back pressure. Equation (6) can be used with figure 31 to determine the engine charge-air flow with satisfactory accuracy. Figure 31, which presents indicated specific air consumption as a unique function of fuel-air ratio, was prepared by use of equation (5) and the same data (table I, tests 242 and 244) that were used in establishing the curve of reference mean effective gas temperature. Data from other tests are included in figure 31.

Equations (5) and (6) can be rewritten to furnish a direct solution for the engine charge-air flow when used with figure 31.

Low blower

$$W_e = \frac{\text{bhp} + 27\left(\frac{N}{1000}\right)^2 - 1.735\left(p_{e_{SL}} - p_{e_{alt}}\right)\left(\frac{N}{1000}\right)}{\frac{1}{W_e/\text{ihp}} - 0.0024\left(\frac{N}{1000}\right)^2} \qquad (7)$$

High blower

$$W_e = \frac{\text{bhp} + 27\left(\frac{N}{1000}\right)^2 - 1.735\left(p_{e_{SL}} - p_{e_{alt}}\right)\left(\frac{N}{1000}\right)}{\frac{1}{W_e/\text{ihp}} - 0.00405\left(\frac{N}{1000}\right)^2} \qquad (8)$$

The foregoing method of estimating the engine charge-air flow is presented because of its simplicity and because it gives results in agreement with experience. Estimation of charge-air flow for a number of test conditions, not tabulated in this report, agreed with the measured values within less than 1 percent difference. Estimation of charge air at low altitude should be very reliable. At very high altitudes and at high power, the estimation of charge air may not be so reliable; however, prediction by this method of charge air required for another large aircraft engine tested in an altitude chamber at 15,000 feet agreed with the measured values (unpublished) within 2 percent. No attempt has been made to extend this method above the critical altitude.

EXAMPLE ILLUSTRATING USE OF ENGINE-COOLING CORRELATION

The application of the cooling correlation is illustrated by the solution of a simple problem:

Determine the variation of hottest cylinder-head temperature with cooling-air pressure drop across the engine for the engine-airplane combination described herein for the following operating conditions: Army summer air, 2000 horsepower, low blower, 2700 rpm, and a fuel-air ratio of 0.107. Assume low airspeed - that is, negligible effect of airspeed on cooling-air temperature.

(1) Estimation of charge air:

From figure 31, at a fuel-air ratio of 0.107,

$$\frac{W_e}{ihp} = 6.43$$

From equation (7),

$$W_e = \frac{2000 + 27(2.7)^2}{\frac{1}{6.43} - 0.0024(2.7)^2}$$

$$= 15900 \text{ lb/hr}$$
$$= 4.42 \text{ lb/sec}$$

(2) Determination of T_g:

From equations (2) and (3),

$$T_g = T_{g_{80}} + 0.8\left[T_e - 80 + 22\left(\frac{N}{1000}\right)^2\right]$$

From figure 18, at a fuel-air ratio of 0.107, read

$$T_{g_{80}} = 882^\circ \text{ F}$$

For Army summer air at sea level,

$$T_e = T_a$$
$$= 100^\circ \text{ F}$$

$$T_g = 882 + 0.8\left[100 - 80 + 22(2.7)^2\right]$$
$$= 1026^\circ \text{ F}$$

(3) Computation of head temperature:

The ratio of temperature differentials $\frac{T_h - T_a}{T_g - T_h}$ is the ordinate.

$$T_h = \frac{(T_g \times \text{Ordinate}) + T_a}{1 + \text{Ordinate}} = \frac{(1026 \times \text{Ordinate}) + 100}{1 + \text{Ordinate}} \qquad (9)$$

For Army summer air at sea level,

$$\sigma = \sigma_a$$
$$= 0.922$$

The column numbers used in the following table refer to:

1. Assumed values of cooling-air pressure drop
2. Computed $W_e^{1.76}/\sigma_a \Delta p$
3. Ordinate from figure 17
4. Average T_h (embedded thermocouples) computed by equation (9)
5. Hottest head-embedded-thermocouple temperature from column 4 and figure 21

1	2	3	4	5	
Δp (in. of water)	$\frac{W_e^{1.76}}{\sigma_a \Delta p}$	Ordinate, $\frac{T_h - T_a}{T_g - T_h}$	Average T_h (°F)	Hottest head temperature (°F)	
				Embedded	Spark-plug gasket
6	2.480	0.761	500	569	562
12	1.240	.608	450	515	493
18	.825	.531	421	483	458
24	.620	.482	402	462	435
30	.495	.448	387	446	417

The calculated hottest cylinder-head temperatures, column 5 of the preceding table, are plotted against cooling-air pressure drop in figure 32. This problem has been simplified by ignoring the adiabatic temperature rise due to flight speed. For application at reasonably great airspeed, account must be taken of this adiabatic temperature rise of the cooling air, which must be added to the specified air temperature. The operating conditions chosen for this problem correspond closely to conditions that might exist at take-off. It can be seen from figure 32 that, with a spark-plug-gasket temperature limit of 500° F, a minimum pressure drop of 11 inches of water is required for cooling the hottest head.

Langley Memorial Aeronautical Laboratory
National Advisory Committee for Aeronautics
Langley Field, Va.

REFERENCES

1. Valentine, E. Floyd: Preliminary Investigation Directed toward Improvement of the NACA Cowling. NACA ARR, April 1942.

2. Pinkel, Benjamin, and Ellerbrock, Herman H., Jr.: Correlation of Cooling Data from an Air-Cooled Cylinder and Several Multicylinder Engines. NACA Rep. No. 683, 1940.

3. Schey, Oscar W., Pinkel, Benjamin, and Ellerbrock, Herman H., Jr.: Correction of Temperatures of Air-Cooled Engine Cylinders for Variation in Engine and Cooling Conditions. NACA Rep. No. 645, 1938.

4. Pinkel, Benjamin: Heat-Transfer Processes in Air-Cooled Engine Cylinders. NACA Rep. No. 612, 1938.

5. Pye, D. R.: The Internal Combustion Engine. Vol. II. The Aero-Engine. Clarendon Press (Oxford), 1934, p. 271.

TABLE I

ENGINE-COOLING CORRELATION DATA - GENERAL

Test	Run	bhp	Engine speed (rpm)	Charge-air flow (lb/hr)	Fuel flow (lb/hr)	Fuel-air ratio	Carburetor temperature (°F)	T_a (°F)	ΔT_g (°F)	Cooling-air flow (lb/sec)
Tests with constant fuel-air ratio										
240	1	1100	2120	8040	640	0.0796	68	96	69	71.0
240	2	1100	2120	7973	646	.0810	70	97	71	67.1
240	3	1100	2120	7987	640	.0802	71	99	72	60.6
240	4	1100	2120	7937	630	.0794	73	100	73	59.7
240	5	1100	2120	7803	630	.0808	73	101	73	55.0
240	6	1100	2120	7770	613	.0788	77	100	77	46.9
240	7	1100	2120	7750	613	.0791	78	97	77	37.3
240	8	1100	2120	7790	615	.0790	81	102	80	60.1
240	9	1100	2120	7677	619	.0806	80	99	79	42.5
240	10	1100	2120	7830	623	.0795	80	102	79	60.4
240	12	1100	2120	7855	613	.0780	71	91	72	60.6
240	13	1100	2120	7743	592	.0765	70	91	71	48.5
240	14	1100	2120	7695	592	.0769	67	92	69	47.7
240	15	1100	2120	7578	565	.0746	70	87	71	33.3
240	16	1100	2120	7708	603	.0782	67	91	69	47.6
241	1	600	2120	4647	347	.0746	70	84	71	42.9
241	2	800	2120	5793	454	.0784	69	85	70	44.0
241	3	990	2120	7013	551	.0785	69	87	70	43.8
241	4	1200	2120	8300	644	.0775	68	88	69	43.8
241	5	600	2120	4613	355	.0769	70	86	71	44.6
Tests with varying fuel-air ratio										
242	1	800	2120	5820	461	0.0801	79	97	78	----
242	2	800	2120	5730	424	.0740	78	98	77	----
242	3	800	2120	5780	394	.0681	80	99	79	----
242	4	800	2120	5840	382	.0655	80	98	79	----
242	5	800	2120	6133	373	.0608	80	98	79	----
242	6	800	2120	6740	385	.0571	81	99	80	----
242	7	800	2120	5770	432	.0748	81	98	80	----
242	8	800	2120	5790	396	.0683	82	99	81	----
242	9	800	2120	7370	390	.0530	78	99	77	----
242	10	800	2120	6187	374	.0603	77	96	77	----
242	11	800	2120	5950	377	.0633	75	94	75	----
242	12	800	2120	5727	405	.0707	72	92	73	----
244	1	1400	2120	10533	1139	.1081	56	79	60	----
244	2	1400	2120	10260	1038	.1011	59	81	62	----
244	3	1400	2120	9853	890	.0904	60	82	63	----
244	4	1110	2120	7697	608	.0791	61	81	64	----
244	5	1100	1749	7608	605	.0795	61	81	39	----
244	6	1040	2501	7688	606	.0788	61	81	95	----
244	7	1630	2400	13117	1490	.1136	61	83	86	----

TABLE II

ENGINE-COOLING CORRELATION DATA - CYLINDER HEADS

Test	Run	$T_{g_{80}}$ (°F)	T_g (°F)	T_h (°F)	$\frac{T_h - T_a}{T_g - T_h}$	$\frac{W_a^{1.14}}{W_e}$	$\sigma_a \Delta p$ (in. of water)	$\frac{W_e^{1.76}}{\sigma_a \Delta p}$
Tests with constant fuel-air ratio								
240	1	1154	1223	331	0.264	57.8	43.0	0.096
240	2	1141	1212	339	.277	54.6	36.9	.110
240	3	1148	1220	353	.293	48.7	31.1	.131
240	4	1154	1227	367	.310	48.1	25.6	.157
240	5	1143	1216	385	.342	44.2	19.3	.203
240	6	1160	1237	408	.372	37.0	13.1	.296
240	7	1157	1234	437	.427	28.8	9.7	.398
240	8	1158	1238	367	.304	49.4	30.8	.126
240	9	1145	1224	403	.370	33.8	14.9	.254
240	10	1154	1233	362	.299	49.7	31.1	.126
240	12	1167	1239	350	.291	49.5	31.4	.126
240	13	1180	1251	374	.323	38.8	19.5	.197
240	14	1176	1245	397	.360	38.4	14.8	.257
240	15	1198	1268	421	.394	25.8	9.5	.390
240	16	1165	1234	396	.364	38.3	14.7	.260
241	1	1198	1268	338	.273	56.2	13.5	.116
241	2	1163	1233	356	.309	46.6	14.5	.159
241	3	1162	1232	383	.349	38.0	14.2	.228
241	4	1171	1240	404	.378	32.1	14.4	.303
241	5	1176	1247	337	.276	59.2	14.2	.109
Tests with varying fuel-air ratio								
242	1	1142	1220	362	0.309	----	14.7	0.159
242	2	1183	1260	368	.303	----	15.0	.151
242	3	1191	1270	374	.307	----	14.8	.155
242	4	1186	1265	373	.308	----	14.9	.157
242	5	1131	1210	366	.318	----	14.8	.172
242	6	1021	1101	350	.334	----	15.0	.201
242	7	1180	1260	371	.307	----	14.9	.154
242	8	1194	1275	376	.308	----	14.8	.156
242	9	926	1003	334	.352	----	14.9	.237
242	10	1108	1185	359	.318	----	15.1	.172
242	11	1161	1236	364	.309	----	15.2	.159
242	12	1182	1255	364	.305	----	15.1	.152
244	1	880	940	337	.429	----	15.1	.438
244	2	913	975	350	.430	----	14.2	.444
244	3	1048	1111	382	.412	----	14.9	.395
244	4	1136	1200	377	.359	----	15.1	.252
244	5	1116	1155	362	.355	----	15.3	.244
244	6	1171	1266	397	.364	----	14.5	.263
244	7	818	904	356	.499	----	13.9	.701

TABLE III

ENGINE-COOLING CORRELATION DATA - CYLINDER BASES

Test	Run	$T_{g_{80}}$ (°F)	T_{g_b} (°F)	T_b (°F)	$\frac{T_b - T_a}{T_g - T_b}$	$\frac{W_a^{1.15}}{W_e}$	$\sigma_a \Delta p$ (in. of water)	$\frac{W_e^{1.67}}{\sigma_a \Delta p}$
Tests with constant fuel-air ratio								
240	1	607	671	244	0.347	60.4	31.6	0.121
240	2	596	667	248	.359	56.9	27.1	.139
240	3	599	671	257	.381	50.4	22.7	.167
240	4	603	676	263	.395	49.9	18.7	.200
240	5	596	669	273	.434	46.1	14.1	.259
240	6	615	682	287	.473	38.4	10.4	.348
240	7	604	681	305	.553	29.7	7.2	.500
240	8	604	684	263	.382	51.3	22.8	.159
240	9	503	676	286	.479	35.2	11.7	.303
240	10	602	681	263	.385	51.5	24.2	.151
240	12	609	681	253	.378	51.4	23.3	.158
240	13	615	686	268	.423	40.4	15.4	.234
240	14	614	683	276	.452	39.8	10.8	.329
240	15	624	695	294	.516	26.8	7.5	.461
240	16	608	677	277	.465	39.7	10.7	.334
241	1	624	695	247	.364	58.1	10.1	.151
241	2	607	677	256	.406	48.2	10.8	.205
241	3	607	677	270	.450	39.5	10.9	.279
241	4	611	680	280	.480	33.4	11.0	.367
241	5	614	685	248	.381	61.6	10.6	.142
Tests with varying fuel-air ratio								
242	1	586	664	260	0.405	----	11.1	0.201
242	2	610	687	263	.389	----	12.6	.173
242	3	601	680	266	.403	----	11.1	.199
242	4	593	672	264	.408	----	11.0	.205
242	5	577	656	262	.416	----	11.1	.220
242	6	538	618	256	.432	----	11.2	.254
242	7	606	686	266	.401	----	11.2	.196
242	8	607	688	268	.403	----	11.1	.199
242	9	507	584	250	.452	----	11.1	.298
242	10	570	646	257	.415	----	11.3	.219
242	11	591	666	259	.407	----	11.4	.204
242	12	607	680	260	.400	----	11.3	.192
244	1	518	578	252	.529	----	11.7	.513
244	2	546	608	262	.525	----	11.4	.504
244	3	584	647	274	.515	----	11.4	.470
244	4	610	674	267	.457	----	11.6	.307
244	5	587	626	250	.451	----	11.8	.296
244	6	657	752	293	.462	----	11.1	.320
244	7	516	602	276	.591	----	11.2	.773

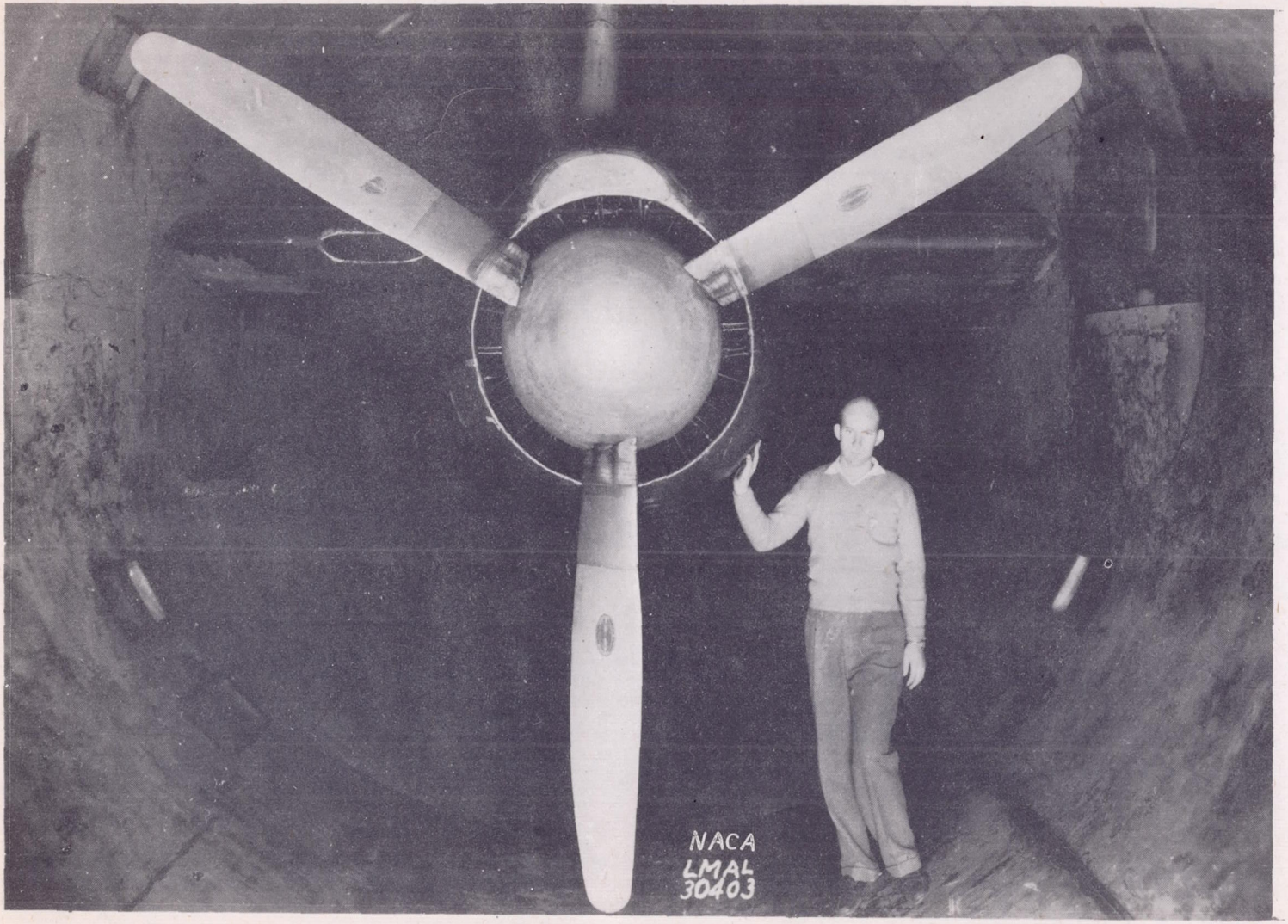

Figure 1.- Wing-nacelle combination in test section of LMAL 16-foot high-speed tunnel.

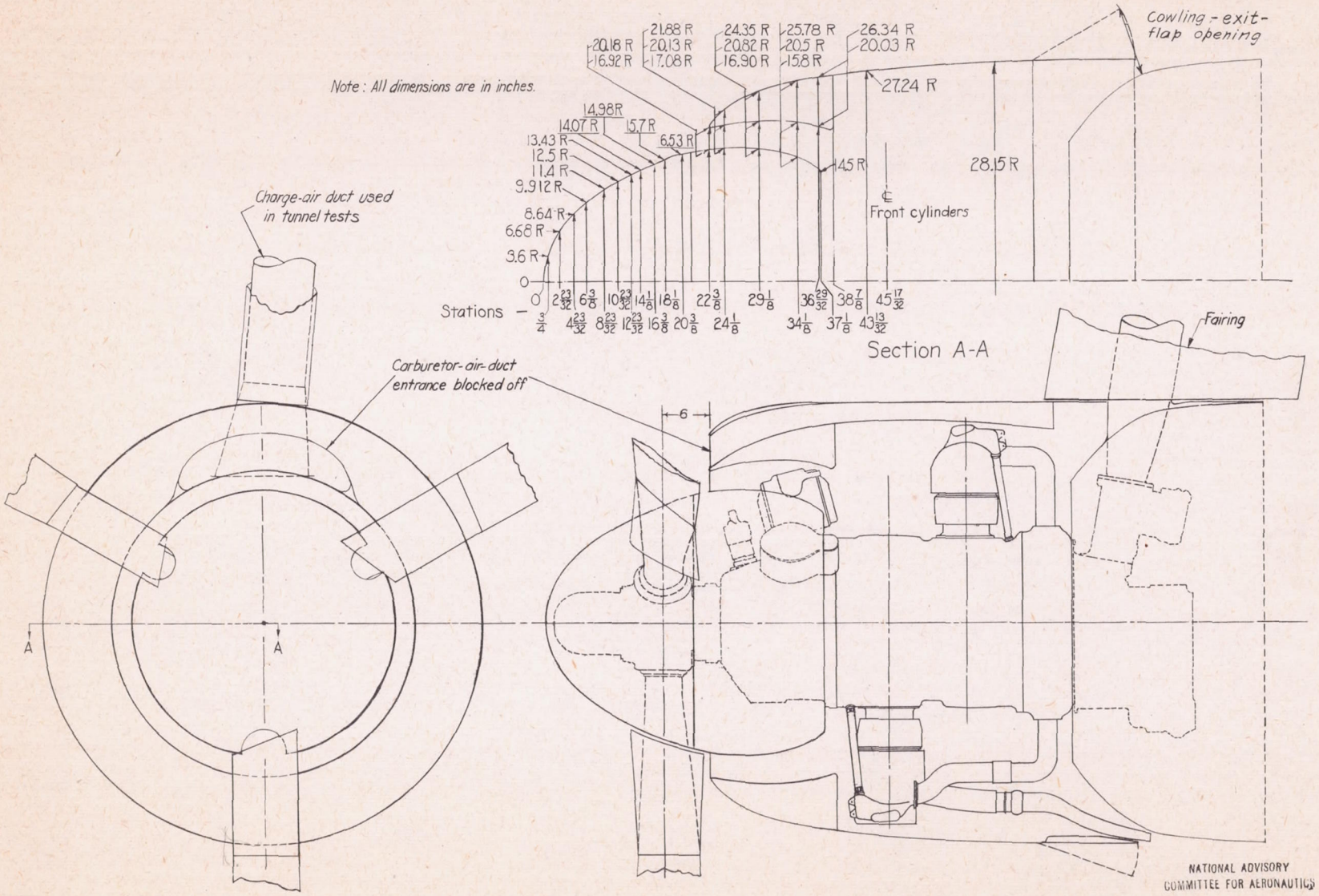

Figure 2.- Outline sketch, NACA D_5 cowling with P.&W. R-2800-B engine.

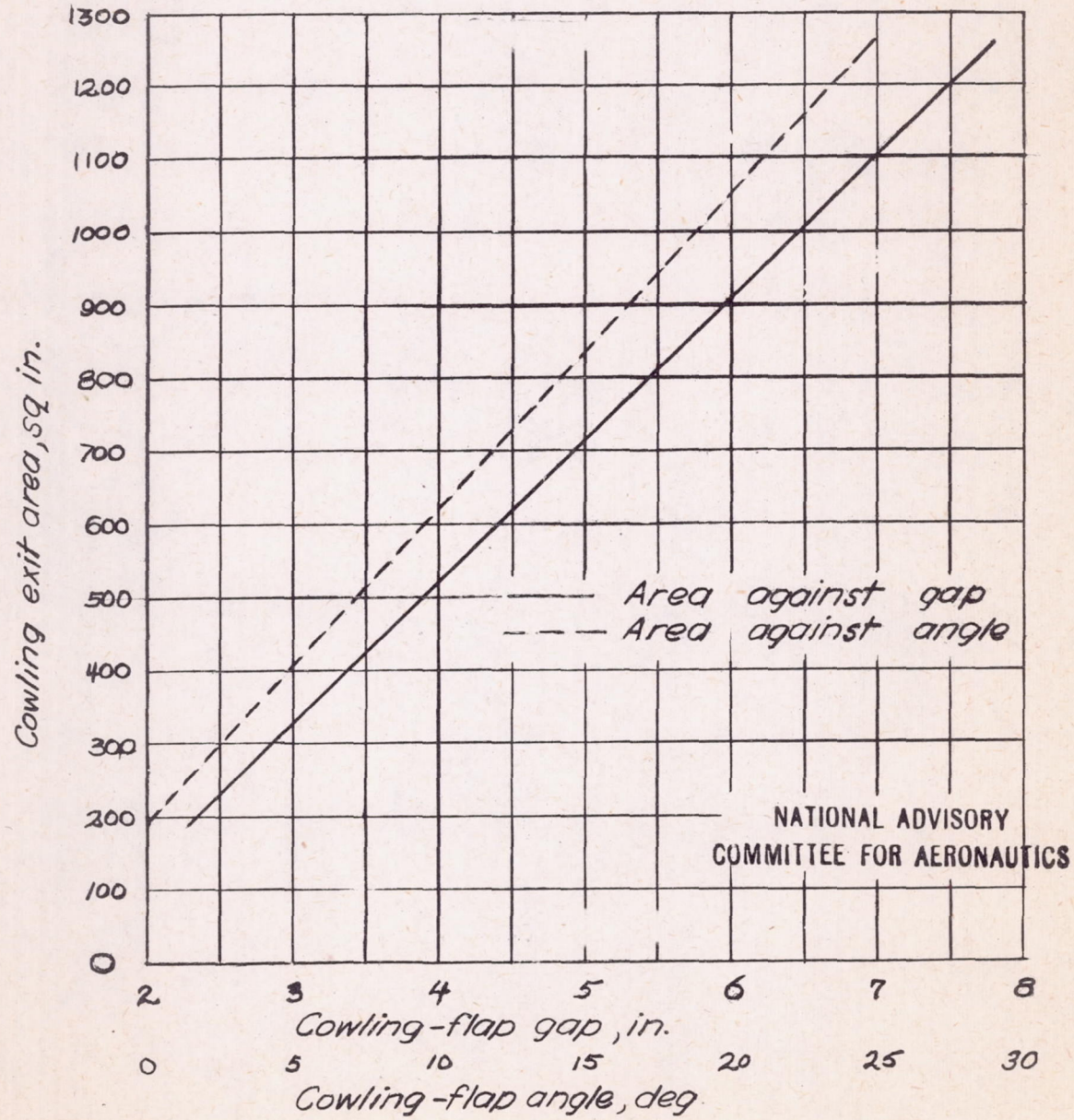

Figure 3. - Cowling-exit-area calibration.

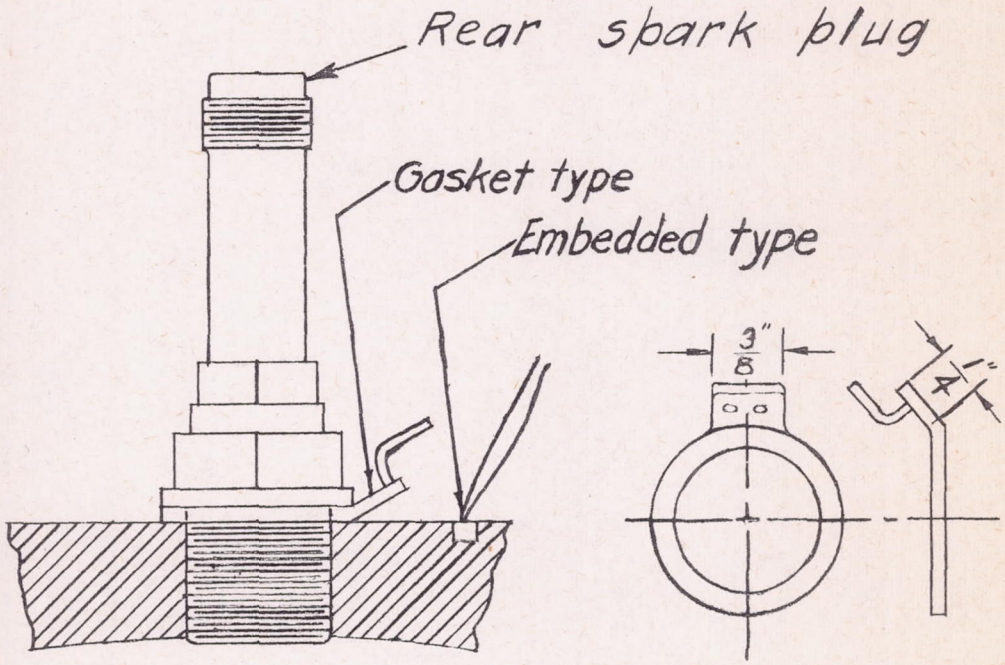

NATIONAL ADVISORY
COMMITTEE FOR AERONAUTICS

Figure 4.-Sketch of cylinder-head thermocouples.

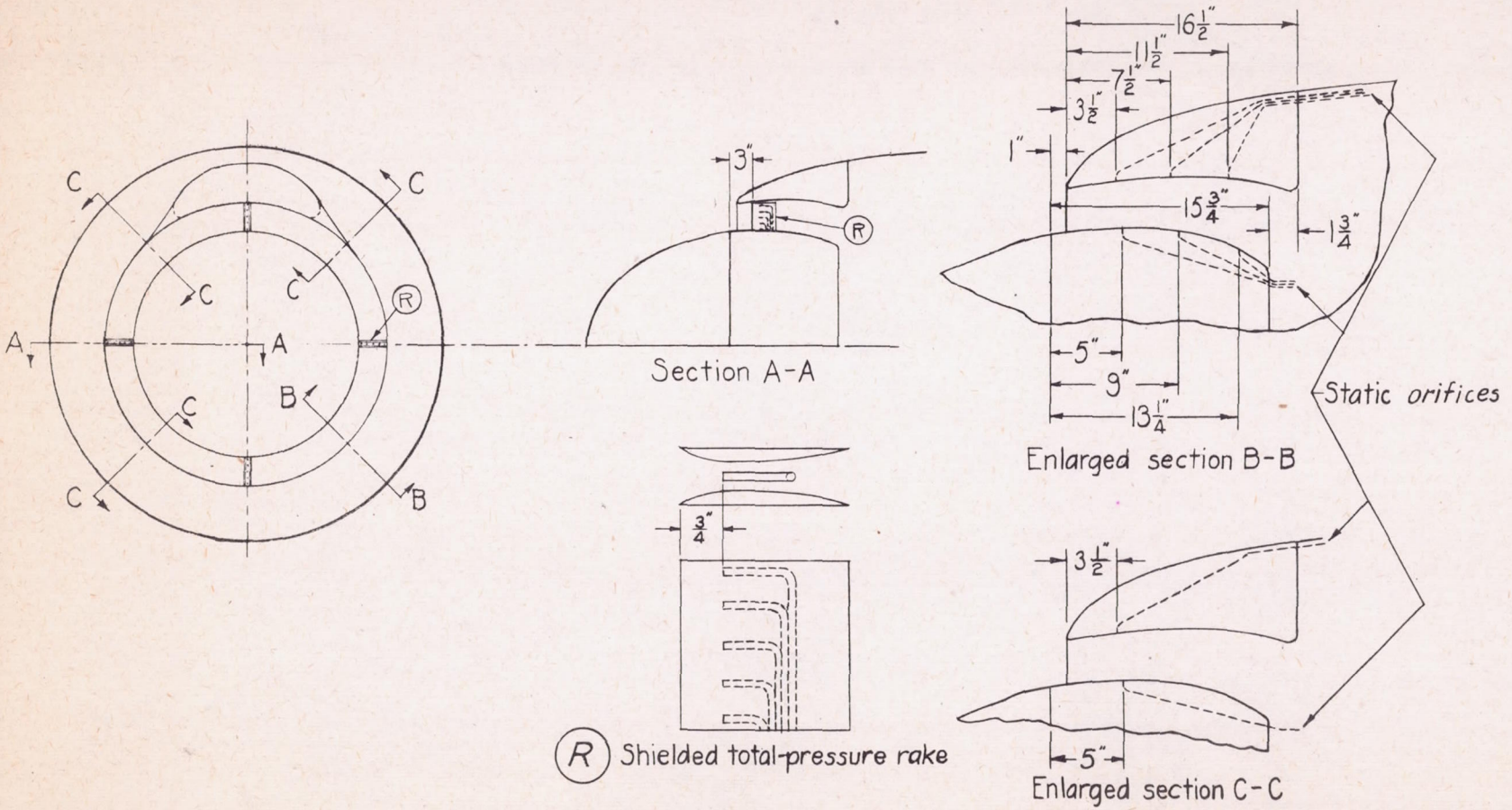

Figure 5.- Pressure-tube locations on fixed spinner and cowling.

NATIONAL ADVISORY
COMMITTEE FOR AERONAUTICS

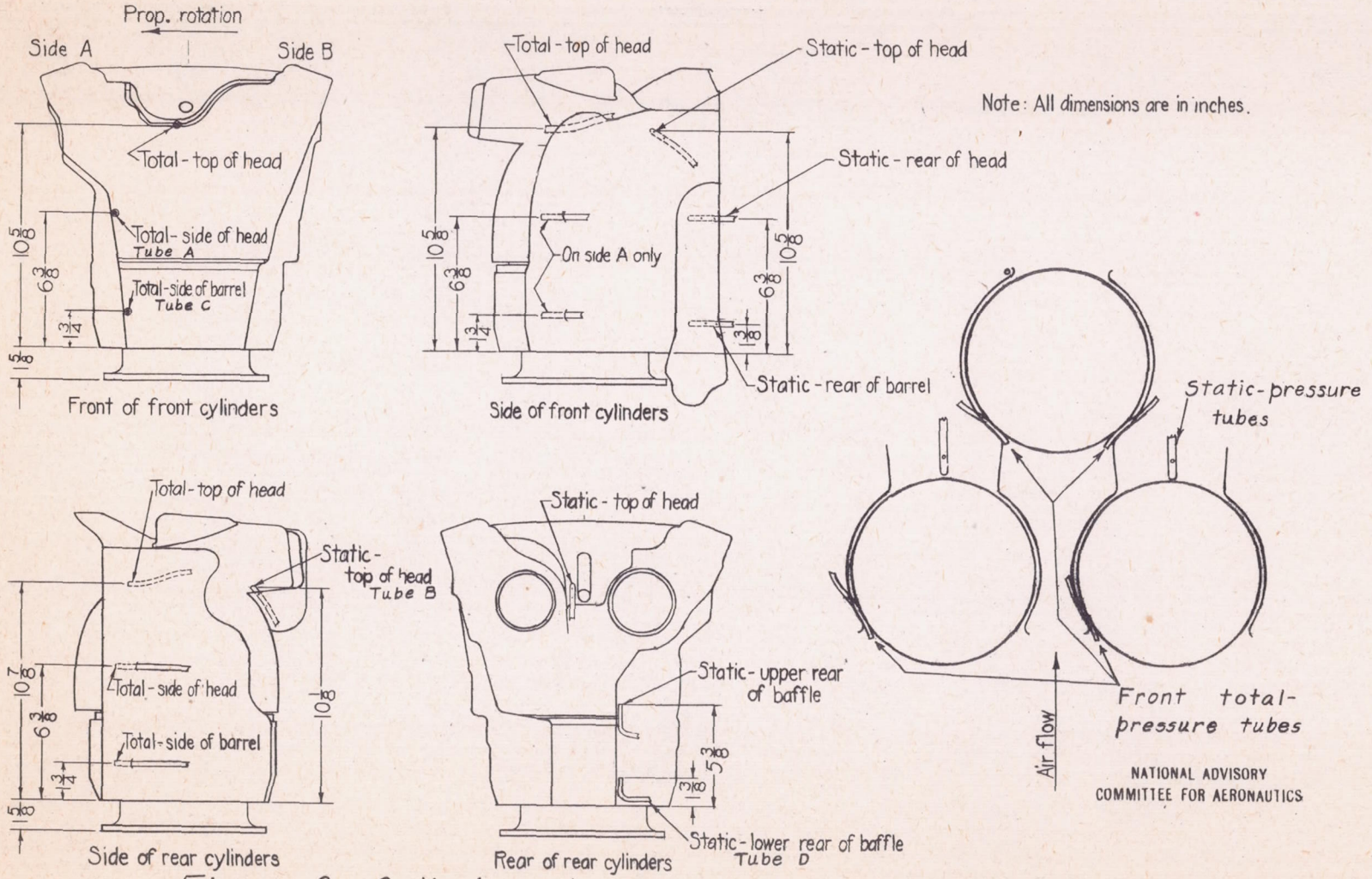

Figure 6.- Cylinder pressure-tube locations.

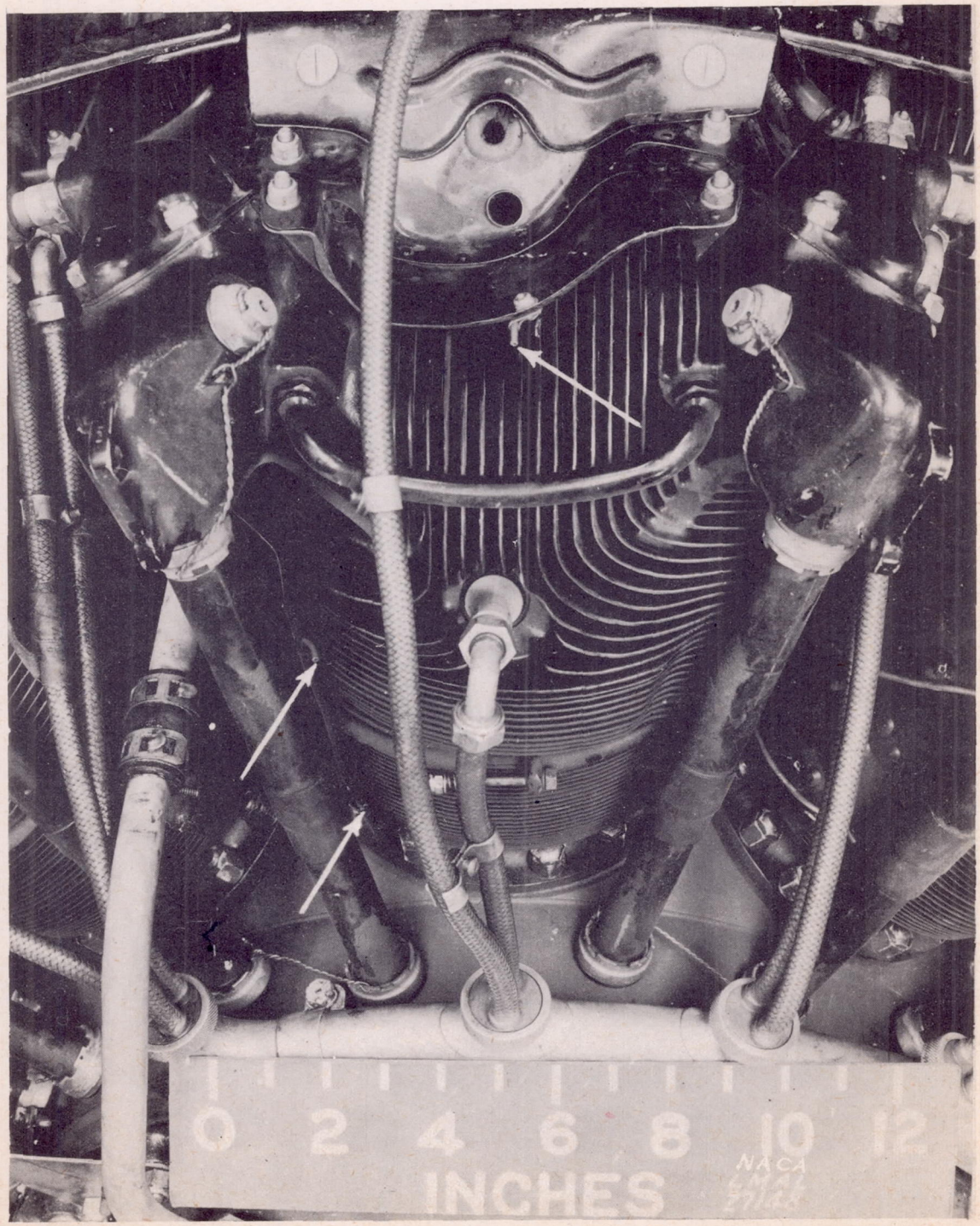

Figure 7.- Pressure-tube locations on front of front cylinders.

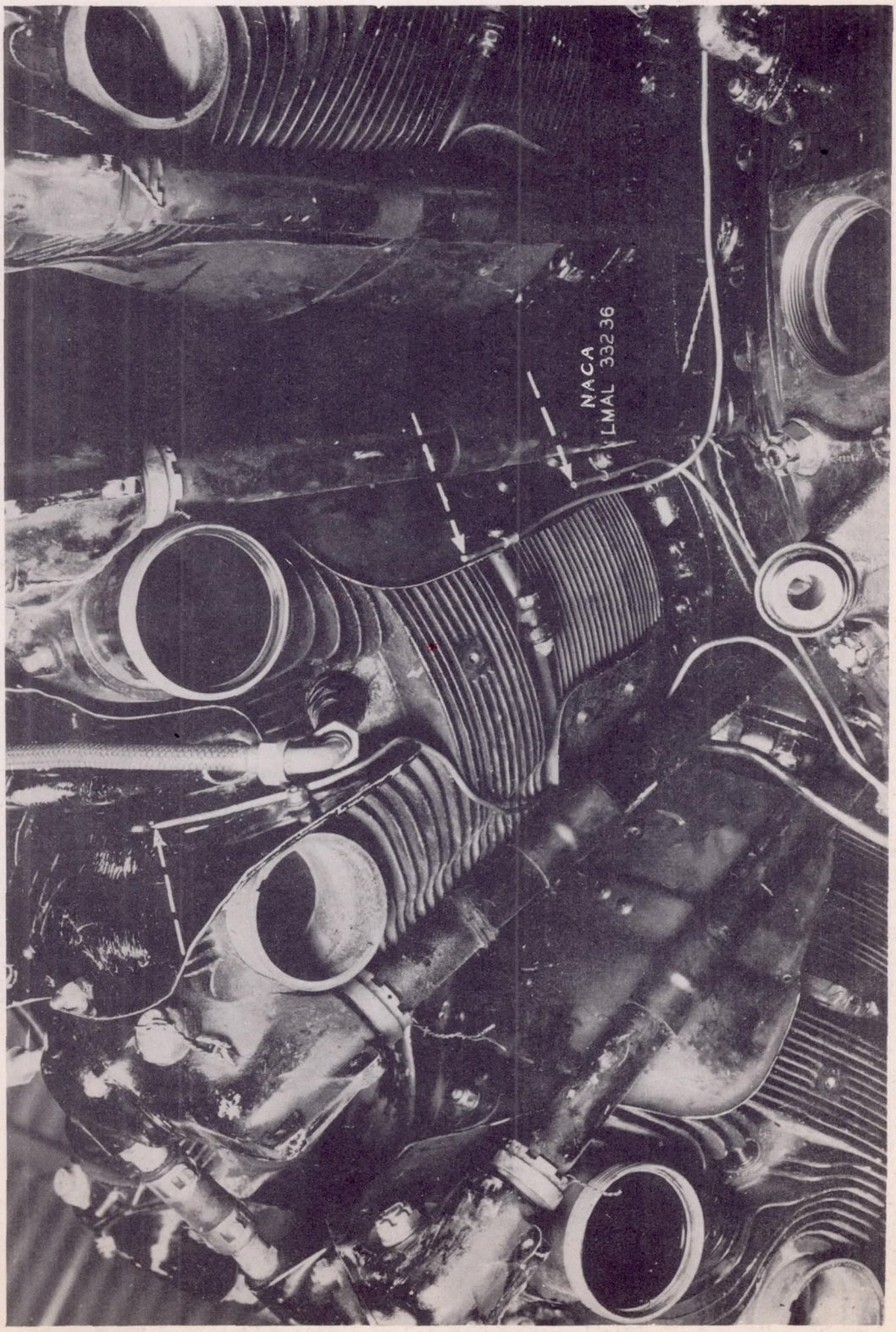

Figure 8.- Pressure-tube locations on rear of rear cylinder.

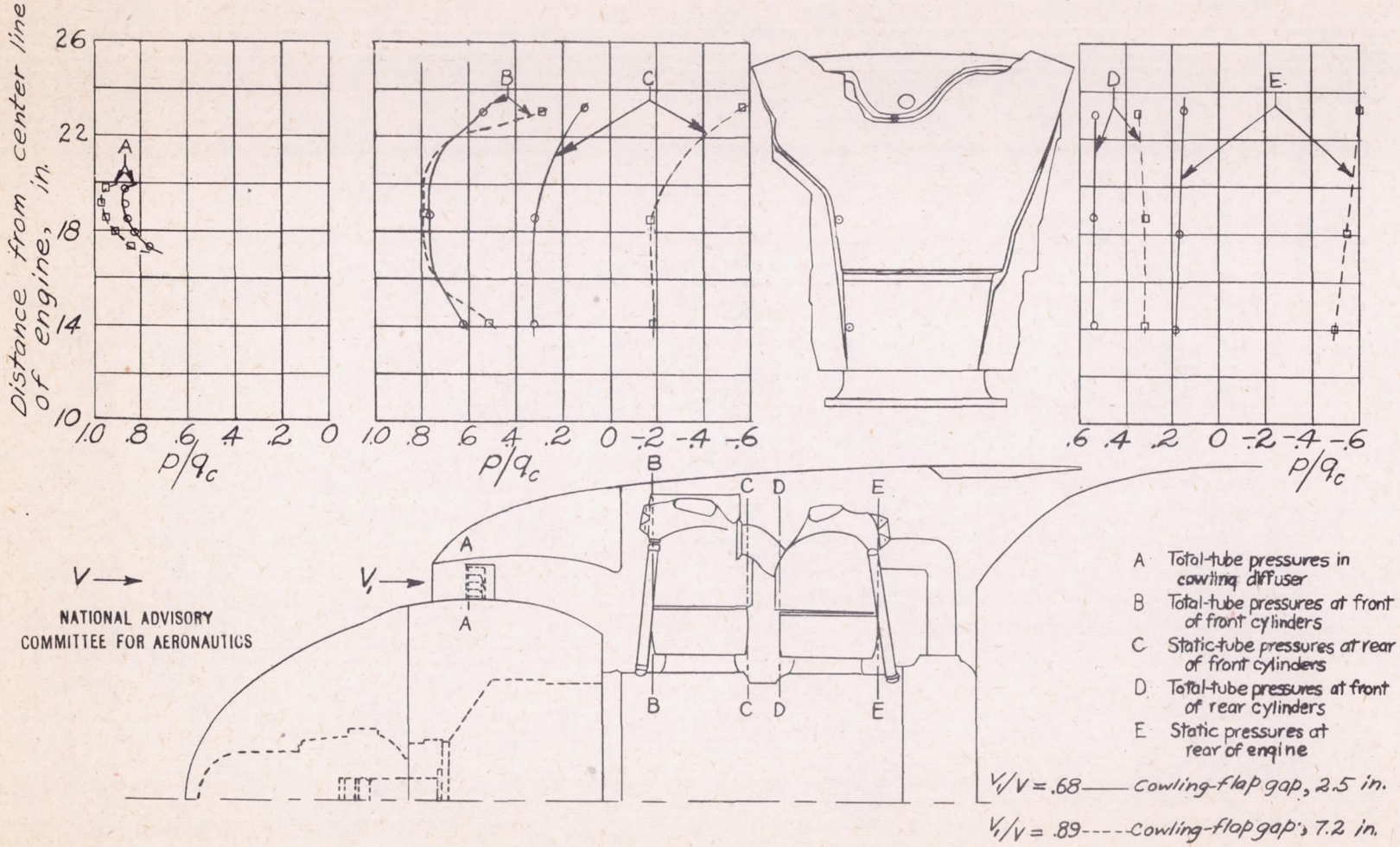

Figure 9.- Typical radial pressure gradients at several locations in the cowling; C_p, 0.20 ; V/nD, 1.9 ; V, 260 m.p.h. ; α_t = 0°; test q_c, 180 lb/sq ft.

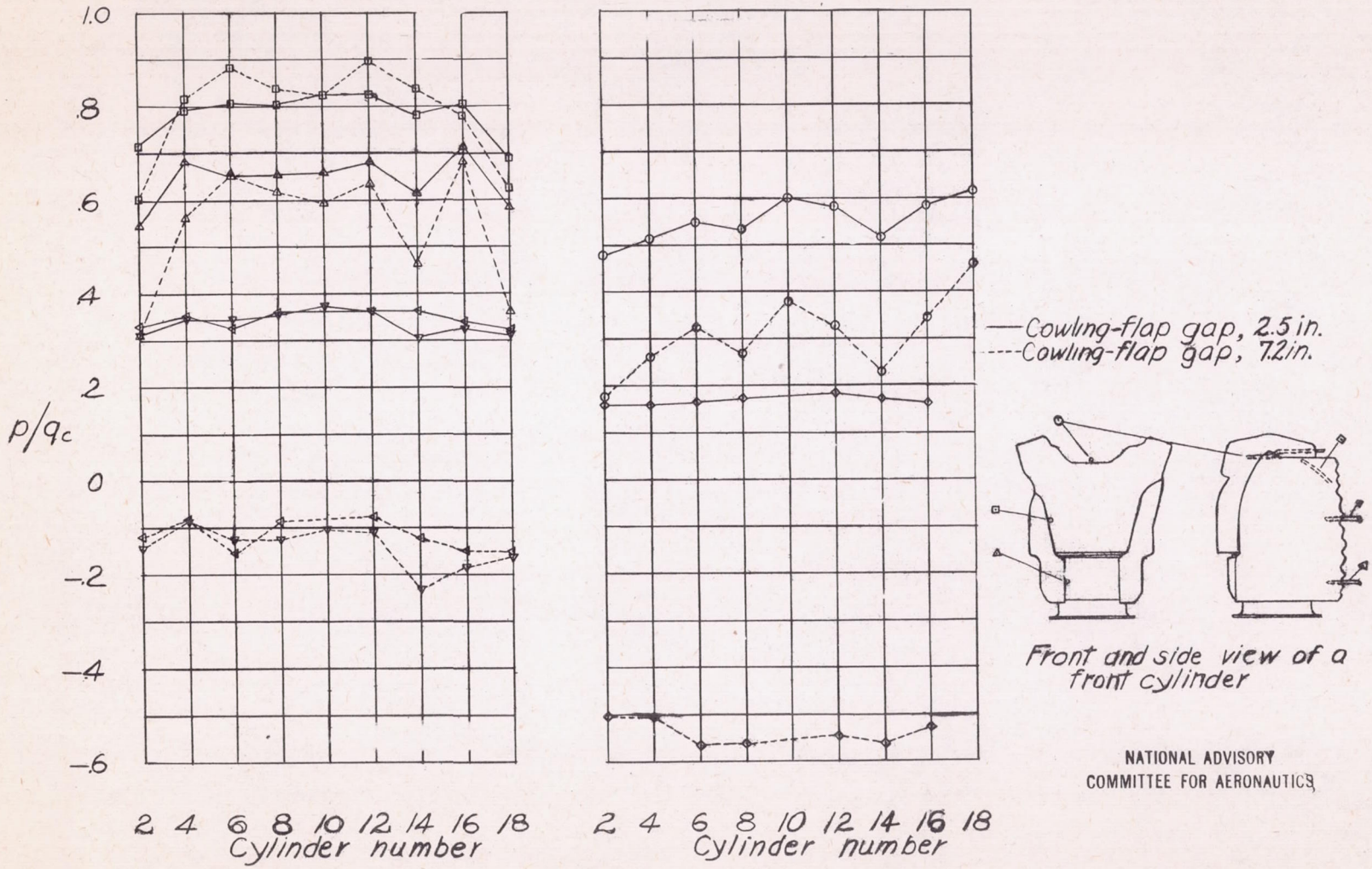

Figure 10.—Circumferential pressure distribution on the front bank of cylinders at 2.5- and 7.2-inch cowling-flap gaps. C_p, 0.20; V/nD, 1.9; V, 260 mph; test q_c, 180 lb/sq ft.

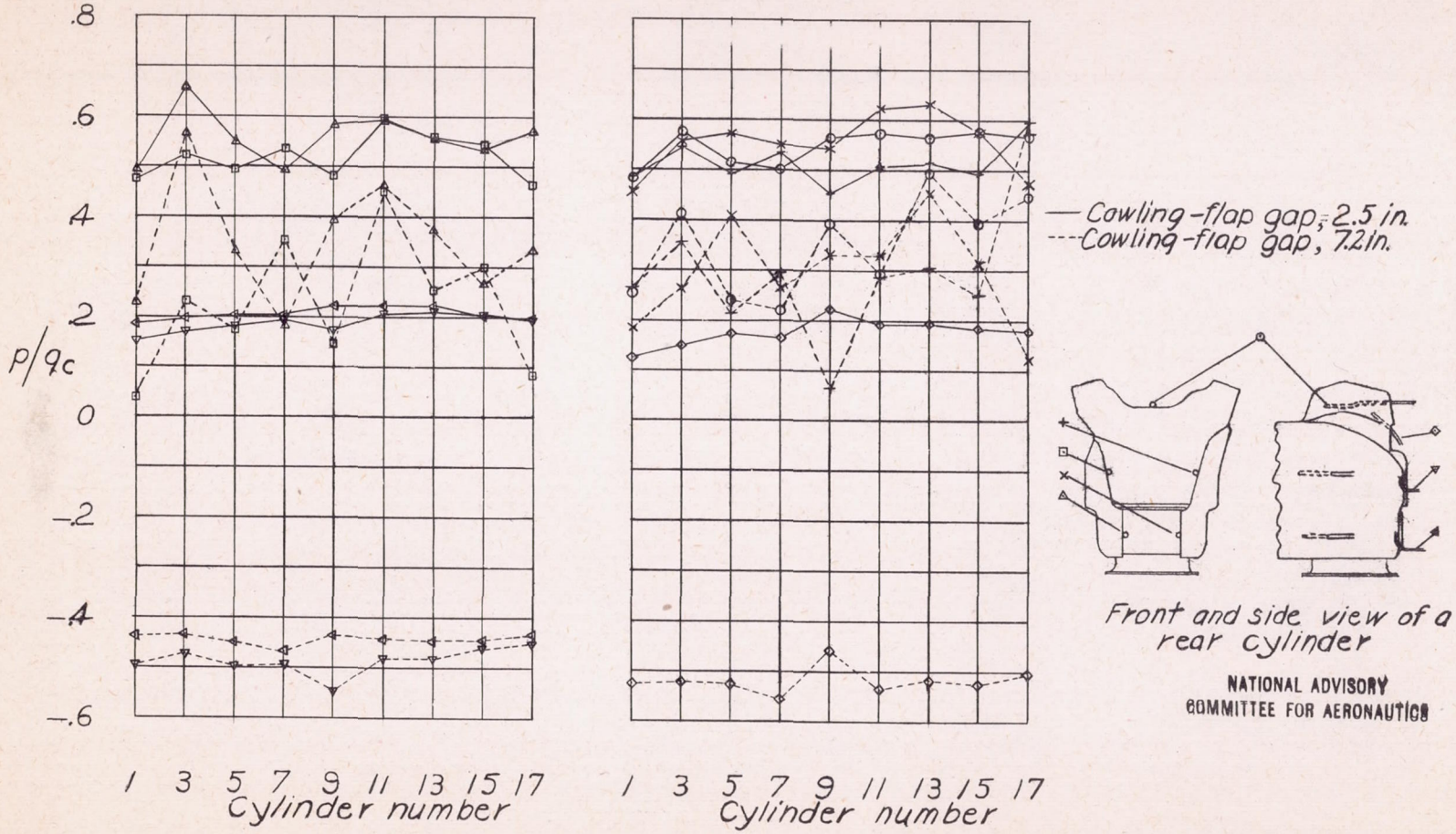

Figure 11.-Circumferential pressure distribution on the rear bank of cylinders at 2.5-and 7.2-inch cowling-flap gaps. C_p, 0.20; V/nD, 1.9 ; V, 260 mph ; test q_c, 180 lb/sq ft.

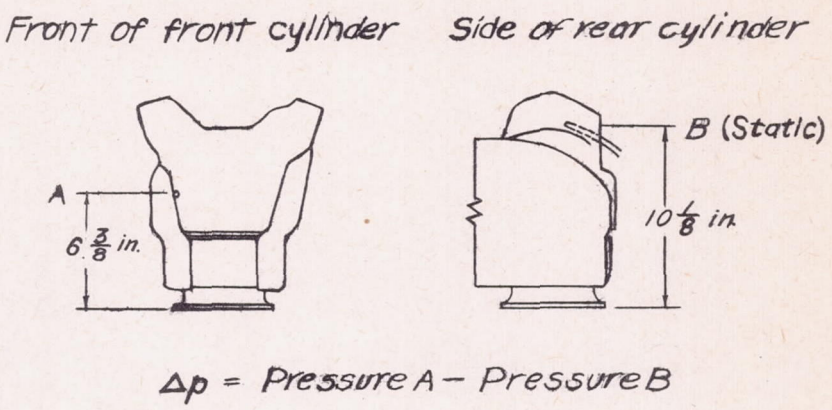

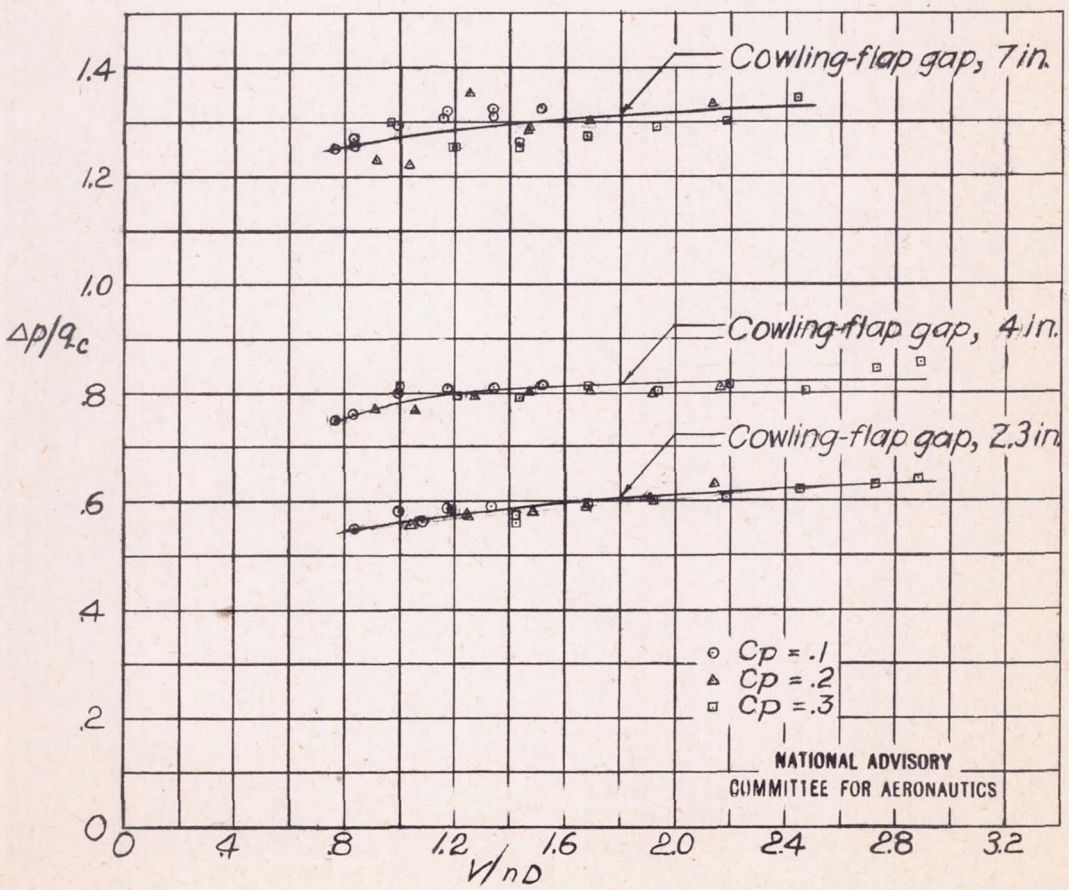

Figure 12.- Variation of available pressure drop across the cylinder heads with propeller-advance ratio.

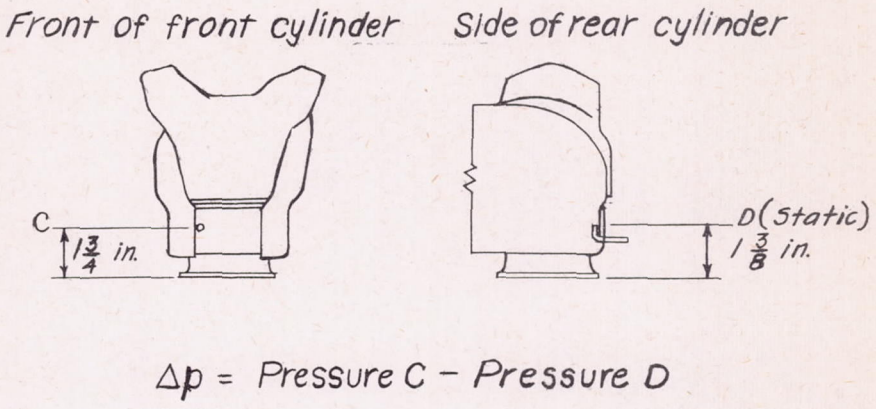

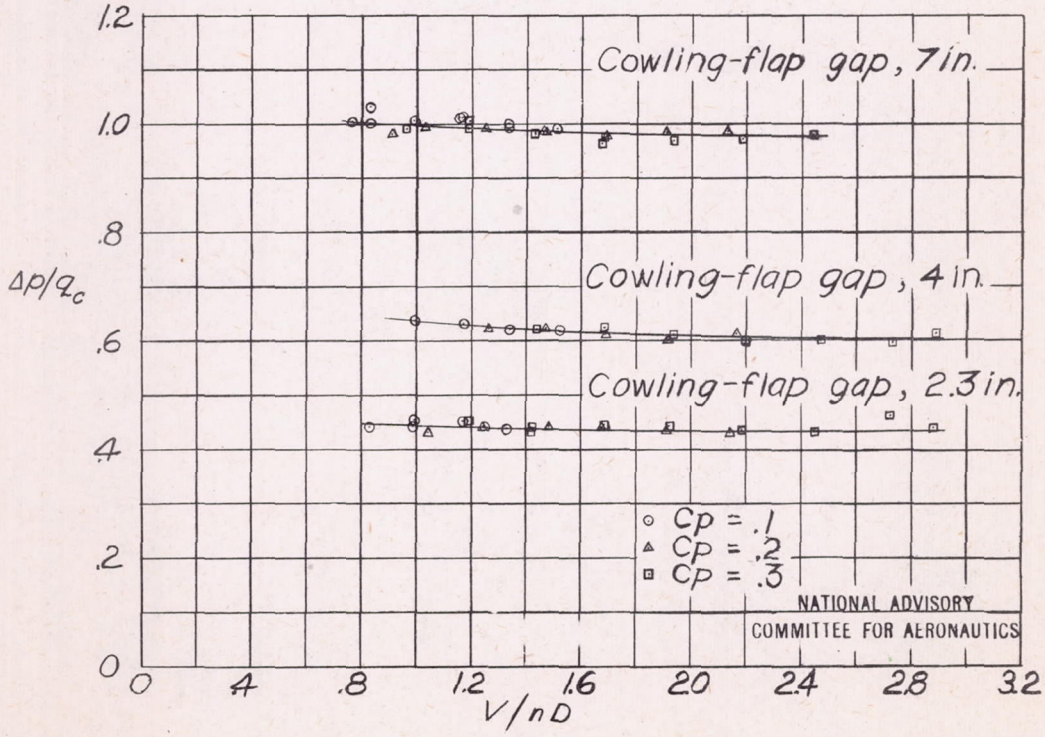

Figure 13.- Variation of available pressure drop across the cylinder barrels with propeller-advance ratio.

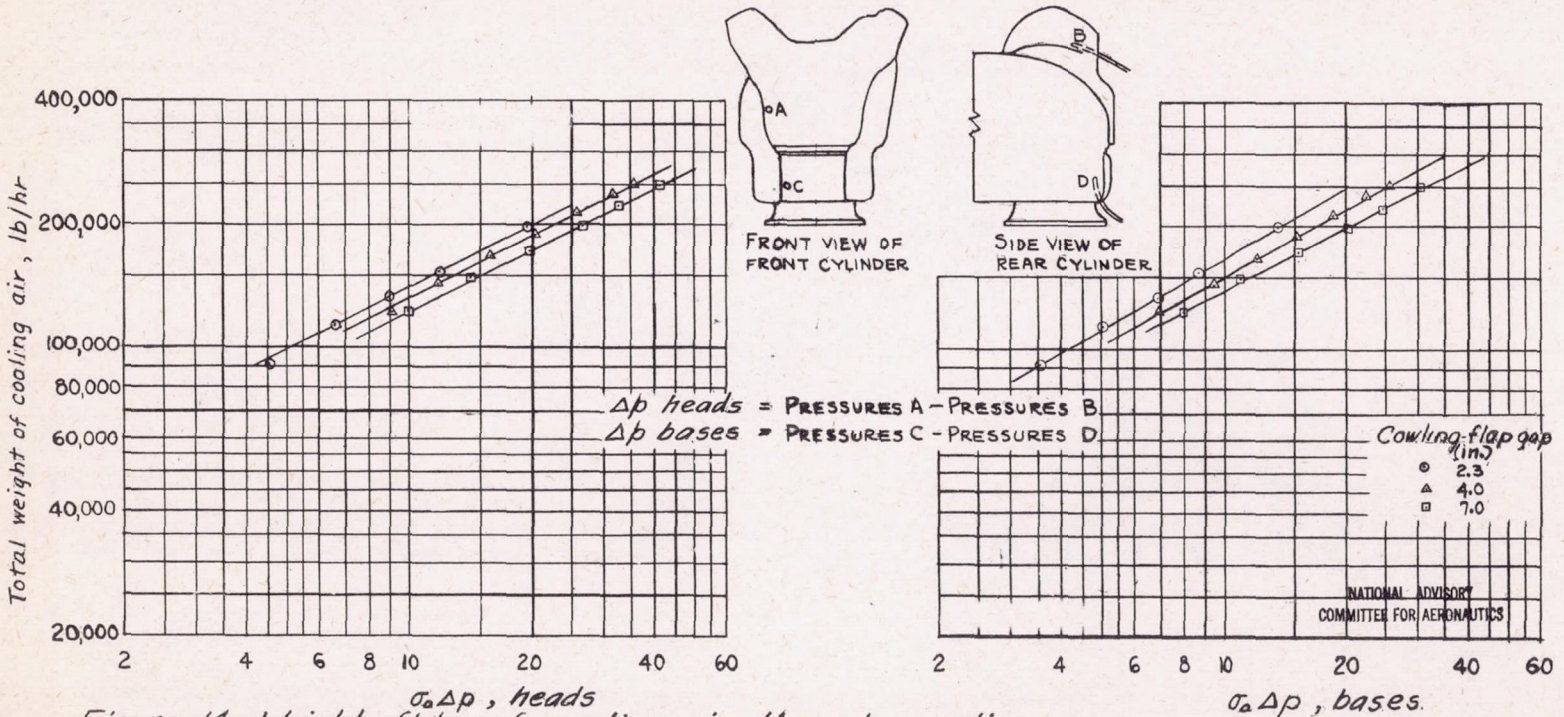

Figure 14.- Weight flow of cooling air through cowling.

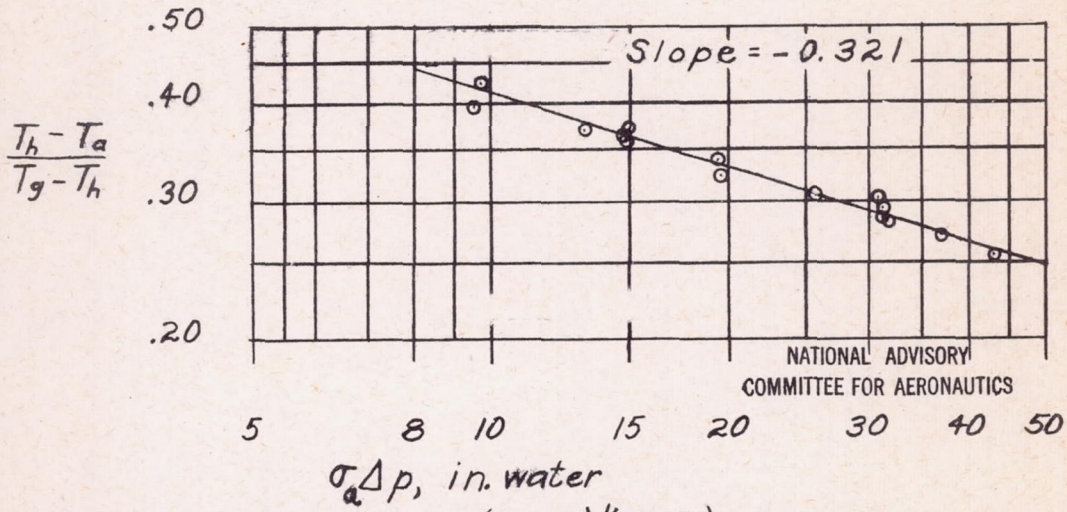

Figure 15. - Variation of $(T_h - T_a)/(T_g - T_h)$ with cooling-air pressure drop. Fuel-air ratio, 0.08; charge-air flow, 7750 pounds per hour. Cylinder heads.

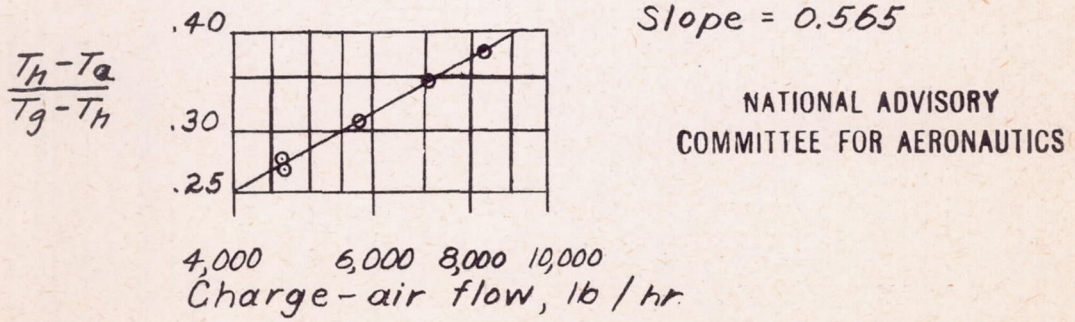

Figure 16. - Variation of $(T_h - T_a)/(T_g - T_h)$ with charge-air flow. Fuel-air ratio, 0.08; $\sigma_a \Delta p$, 14.2 inches of water. Cylinder heads.

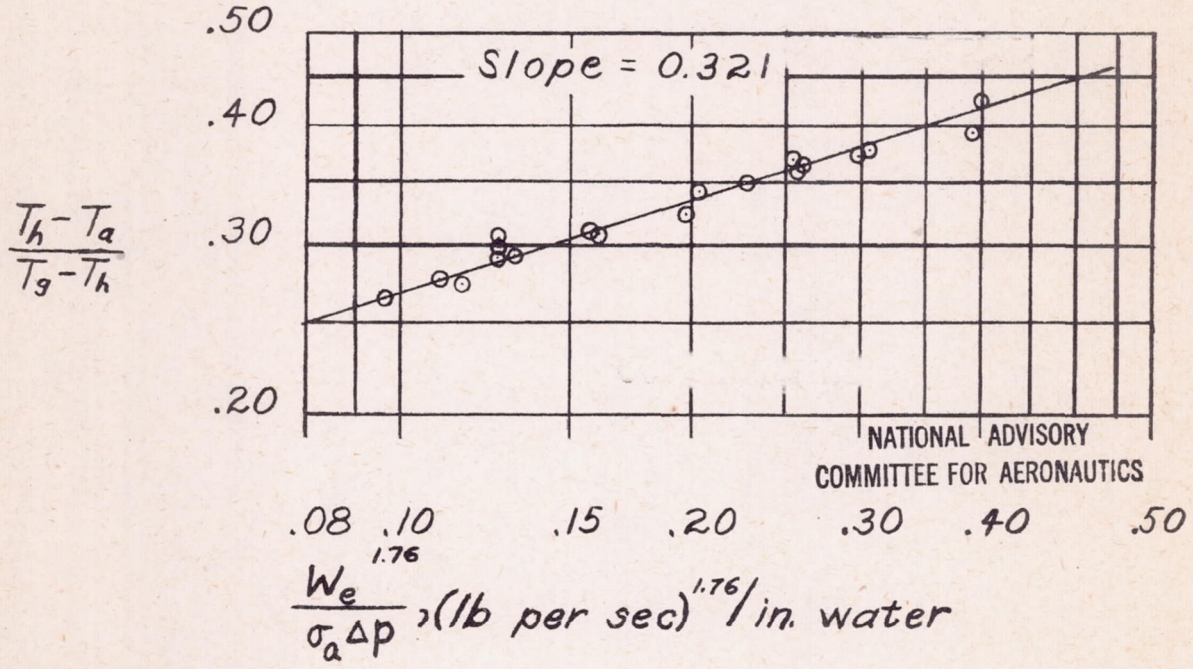

Figure 17.—Cooling correlation based on cooling-air pressure drop. Cylinder heads.

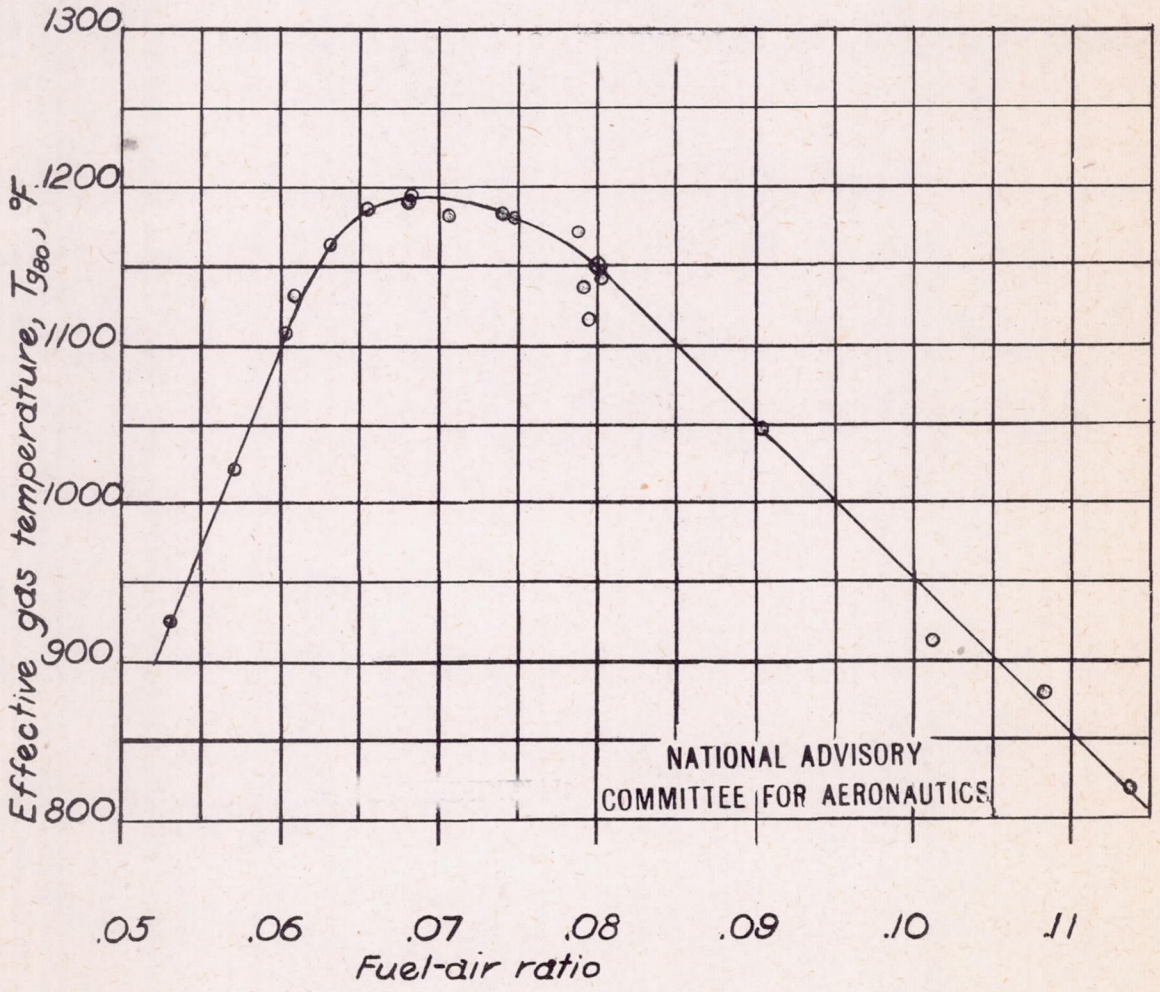

Figure 18. -Variation of mean effective gas temperature with fuel-air ratio. Cylinder heads.

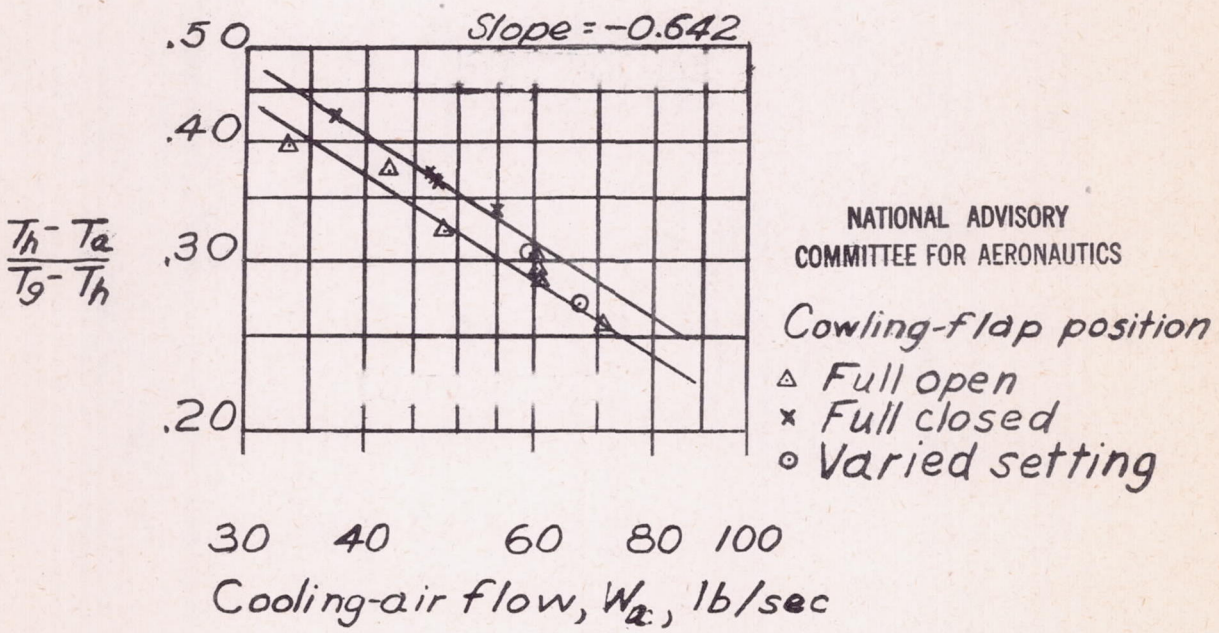

Figure 19.- Variation of $(T_h - T_a)/(T_g - T_h)$ with cooling-air flow. Cylinder heads; charge-air flow, 7750 pounds per hour.

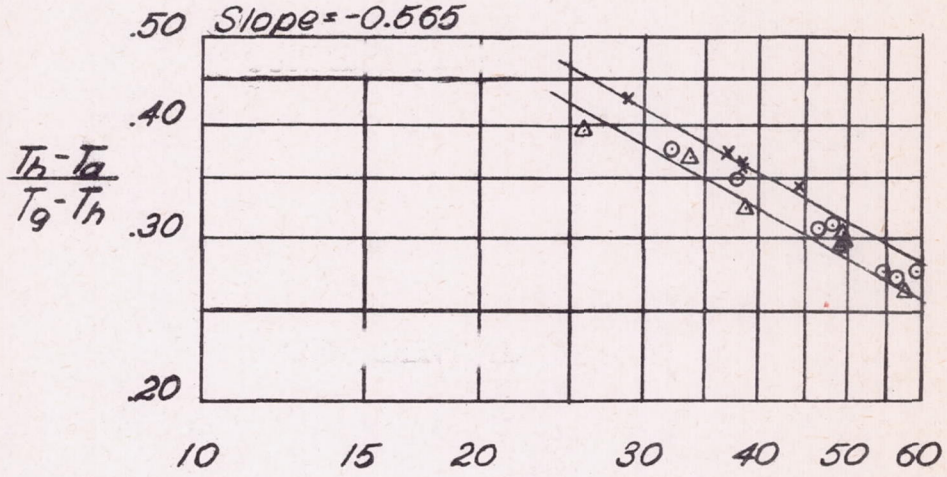

NATIONAL ADVISORY
COMMITTEE FOR AERONAUTICS

Figure 20.—Cooling correlation based on cooling-air weight flow. Cylinder heads.

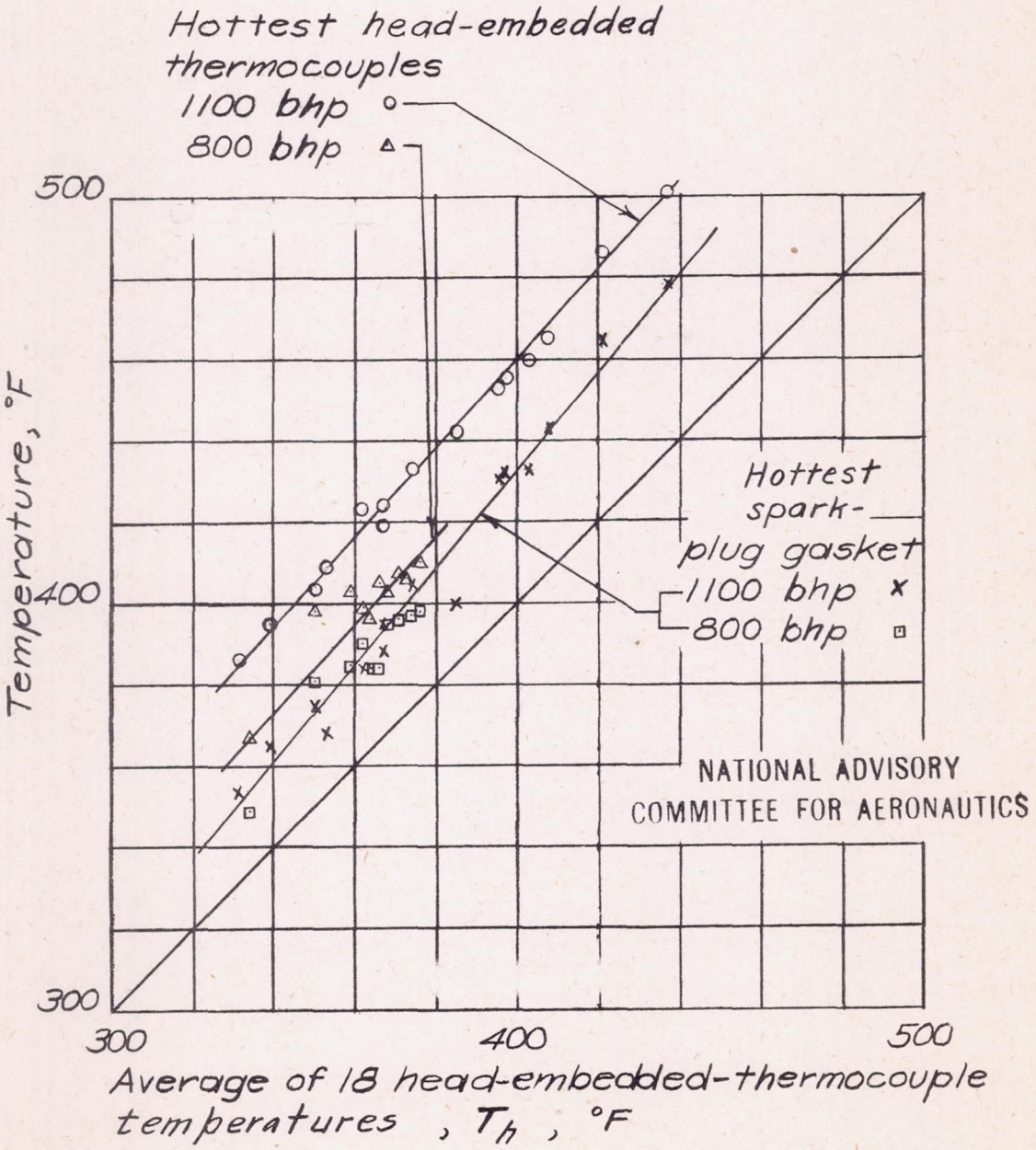

Figure 21. - A comparison of hottest with average head temperatures.

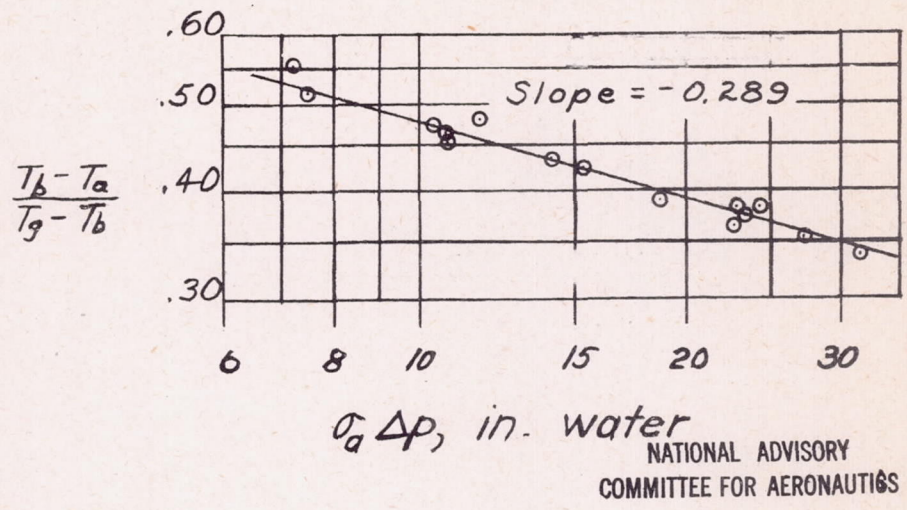

Figure 22.- Variation of $(T_b - T_a)/(T_g - T_b)$ with cooling-air pressure drop. Fuel-air ratio, 0.08; charge-air flow, 7750 pounds per hour. Cylinder bases.

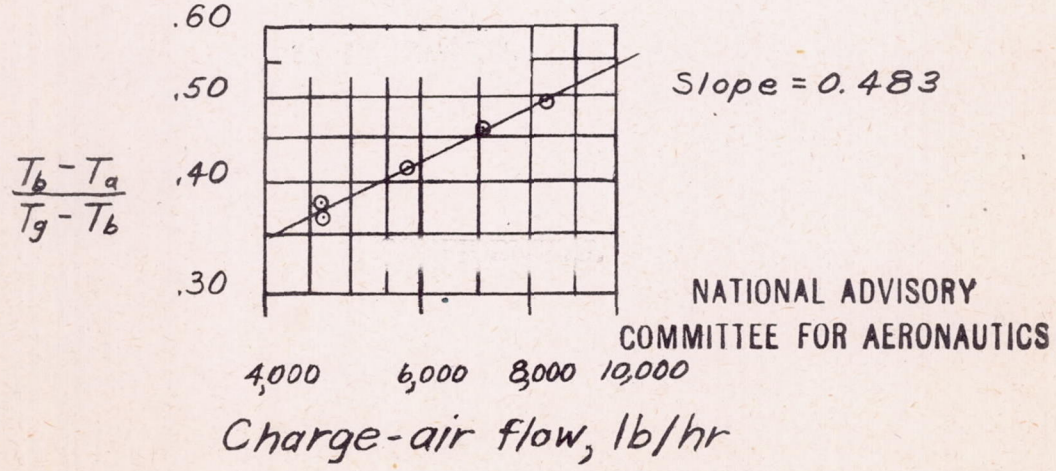

Figure 23.- Variation of $(T_b - T_a)/(T_g - T_b)$ with charge-air flow. Fuel-air ratio, 0.08; $\sigma_a \Delta p$, 10.5 inches of water. Cylinder bases.

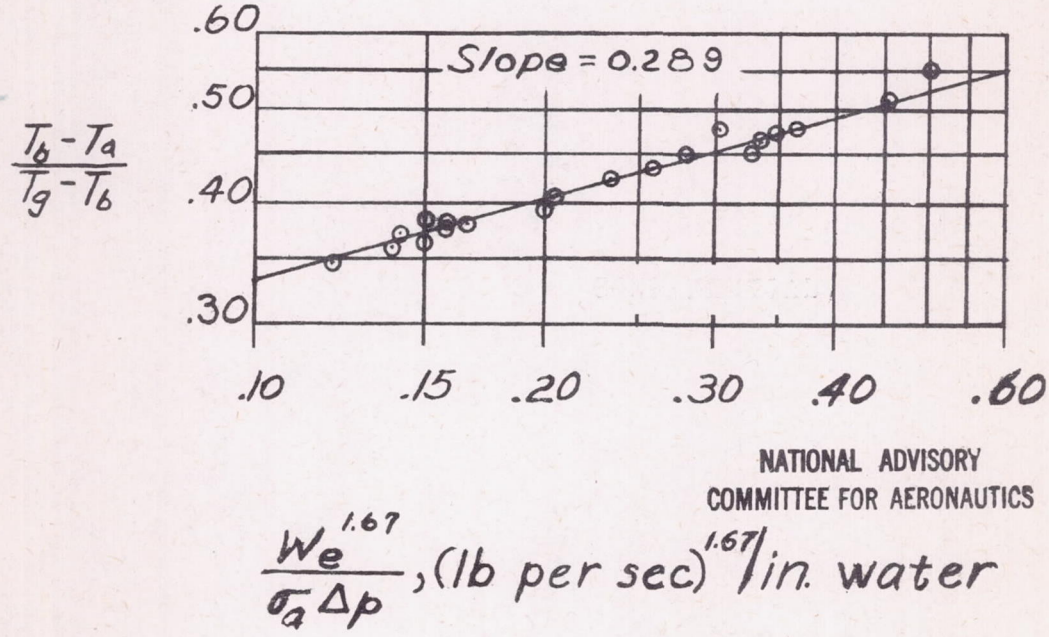

Figure 24.–Cooling correlation based on cooling-air pressure drop. Cylinder bases.

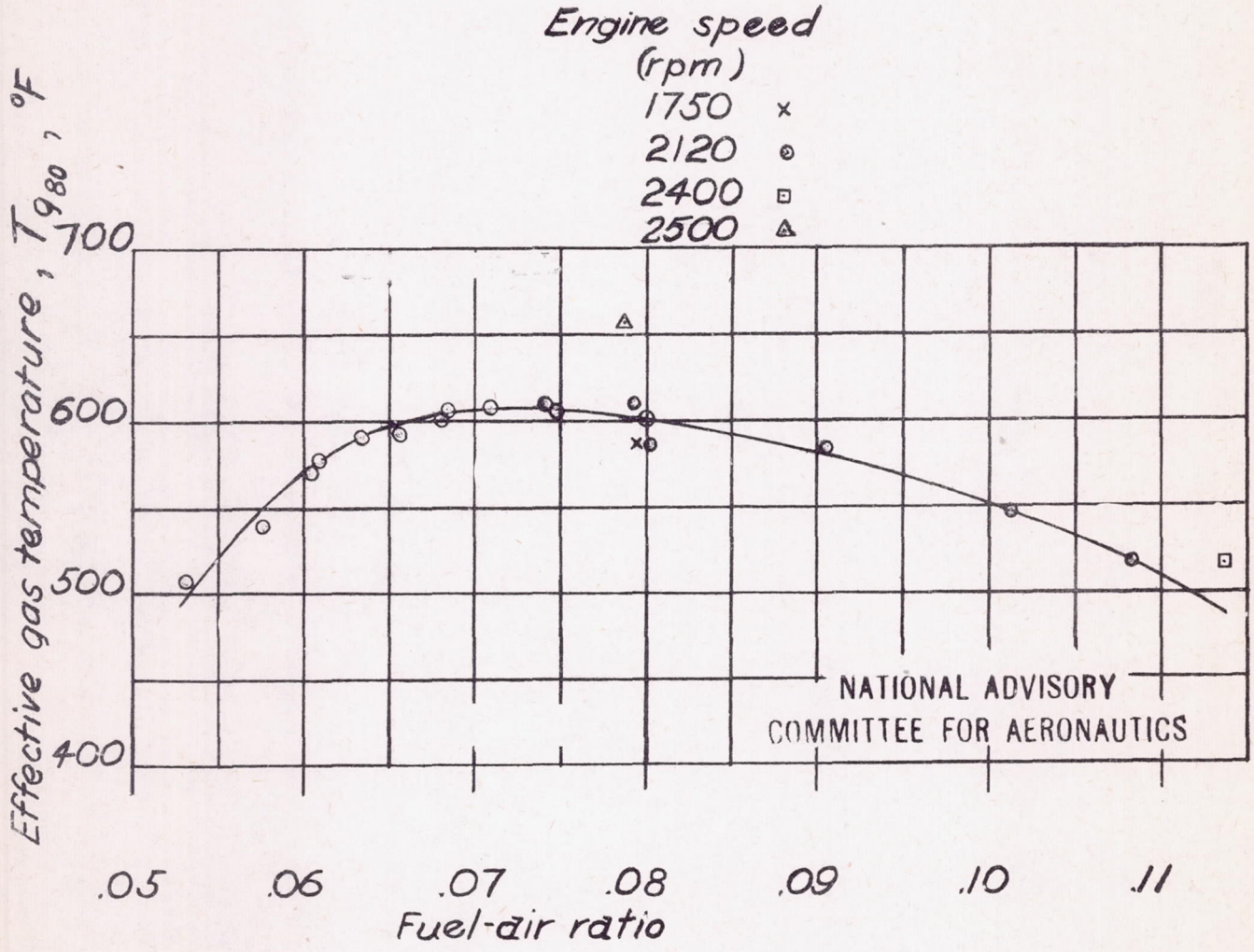

Figure 25.-Variation of mean effective gas temperature with fuel-air ratio. Cylinder bases.

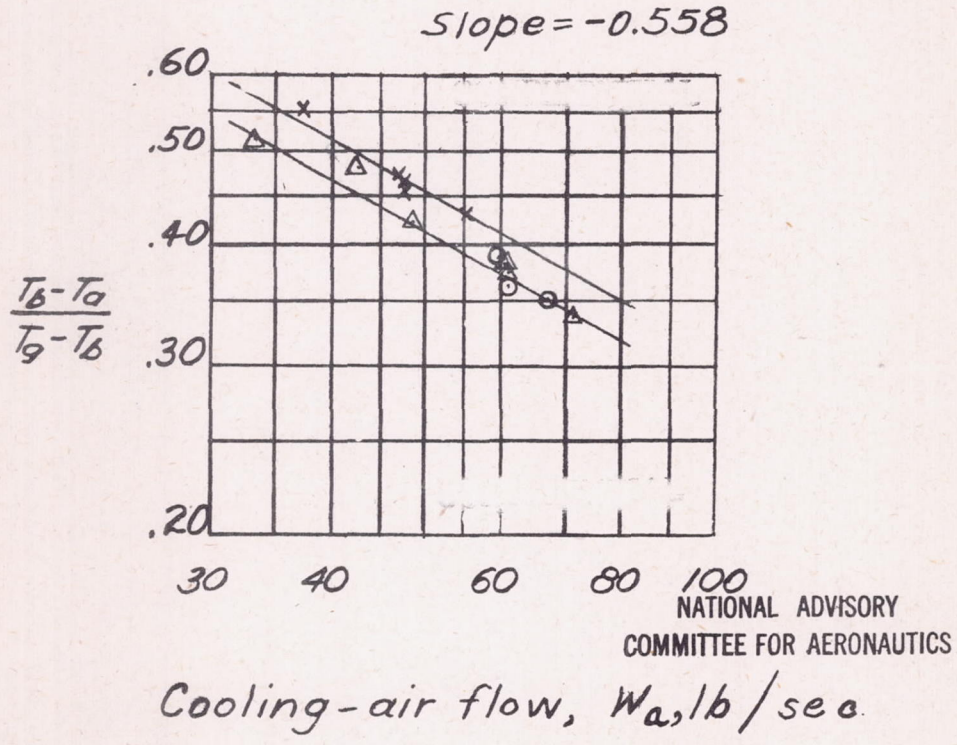

Figure 26.- Variation of $(T_b - T_a)/(T_g - T_b)$ with cooling-air flow. Cylinder bases.

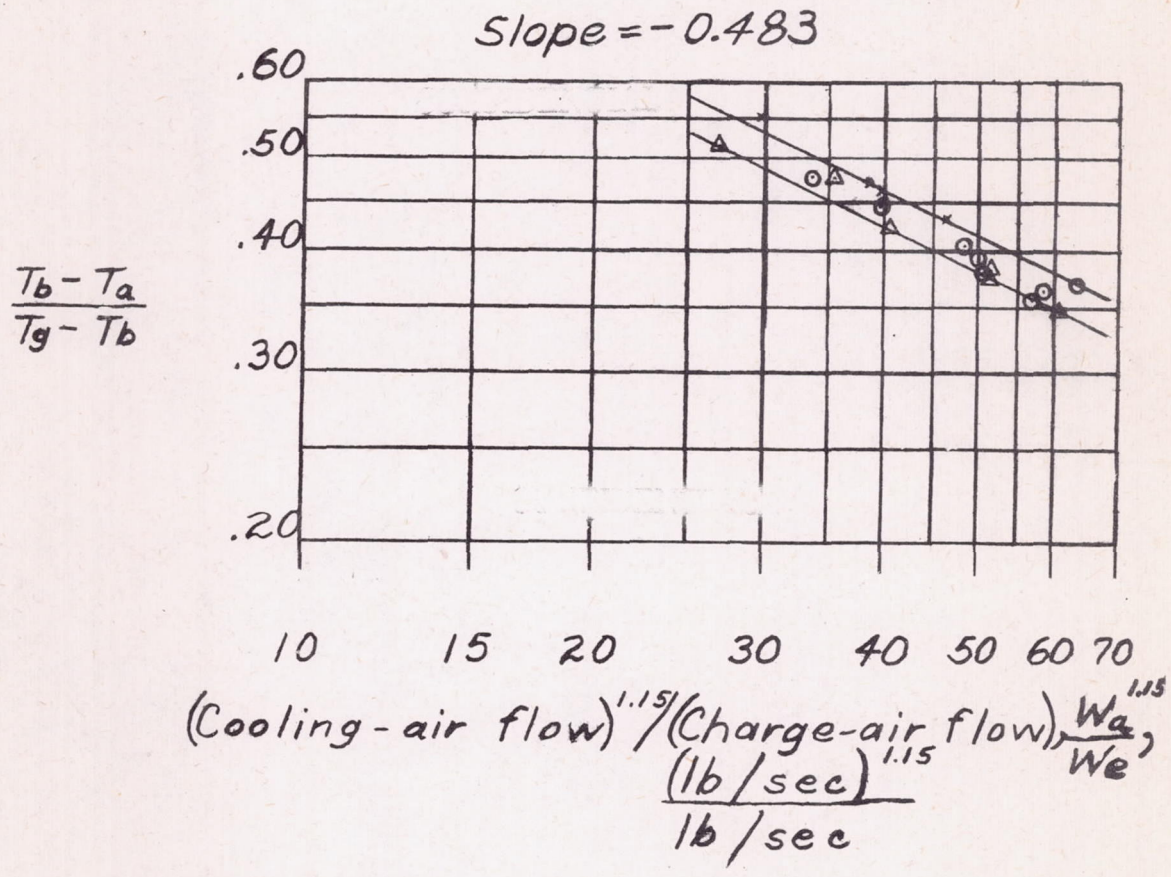

Figure 27.-Cooling correlation based on cooling-air weight flow. Cylinder bases.

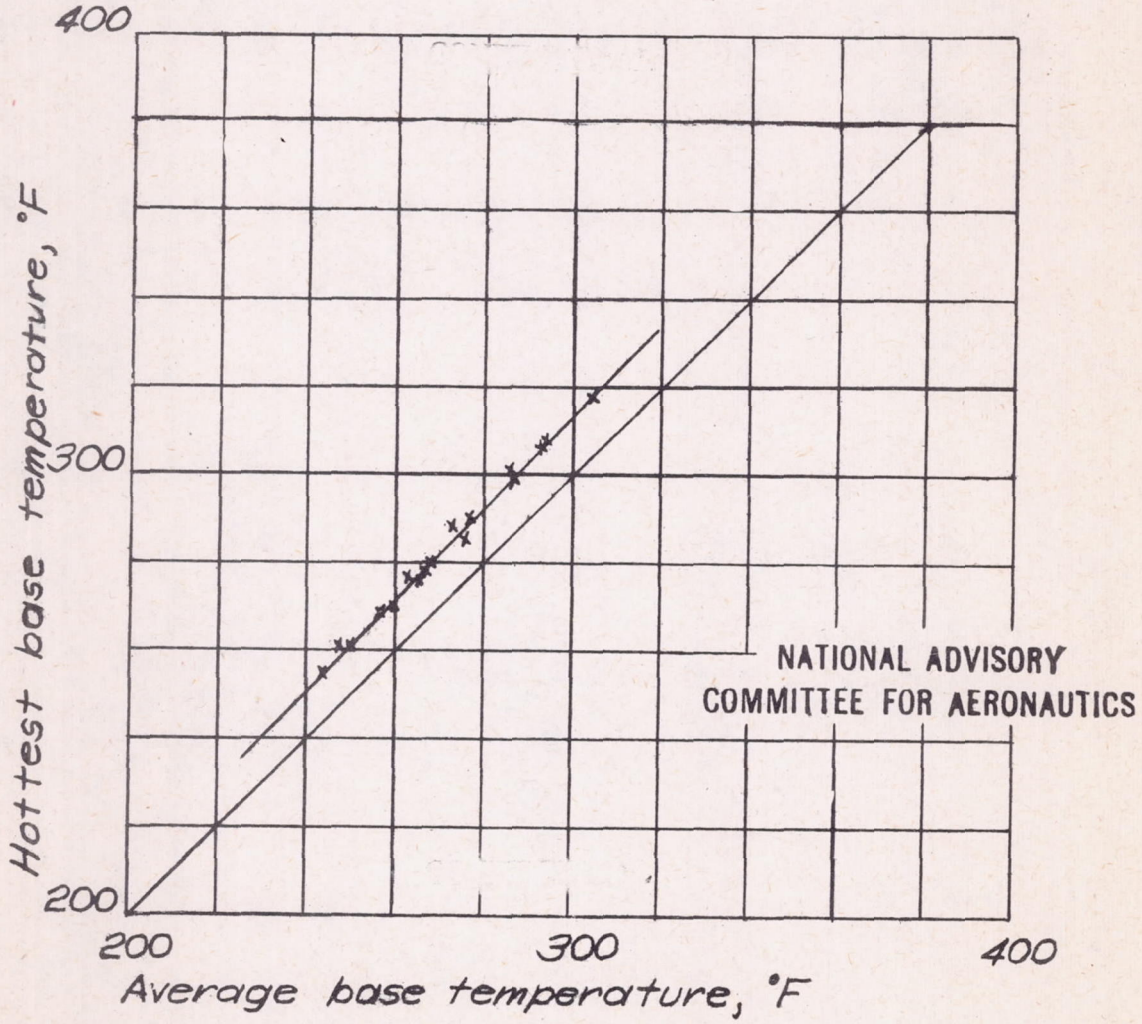

Figure 28.—Comparison of the hottest base temperature with average base temperature.

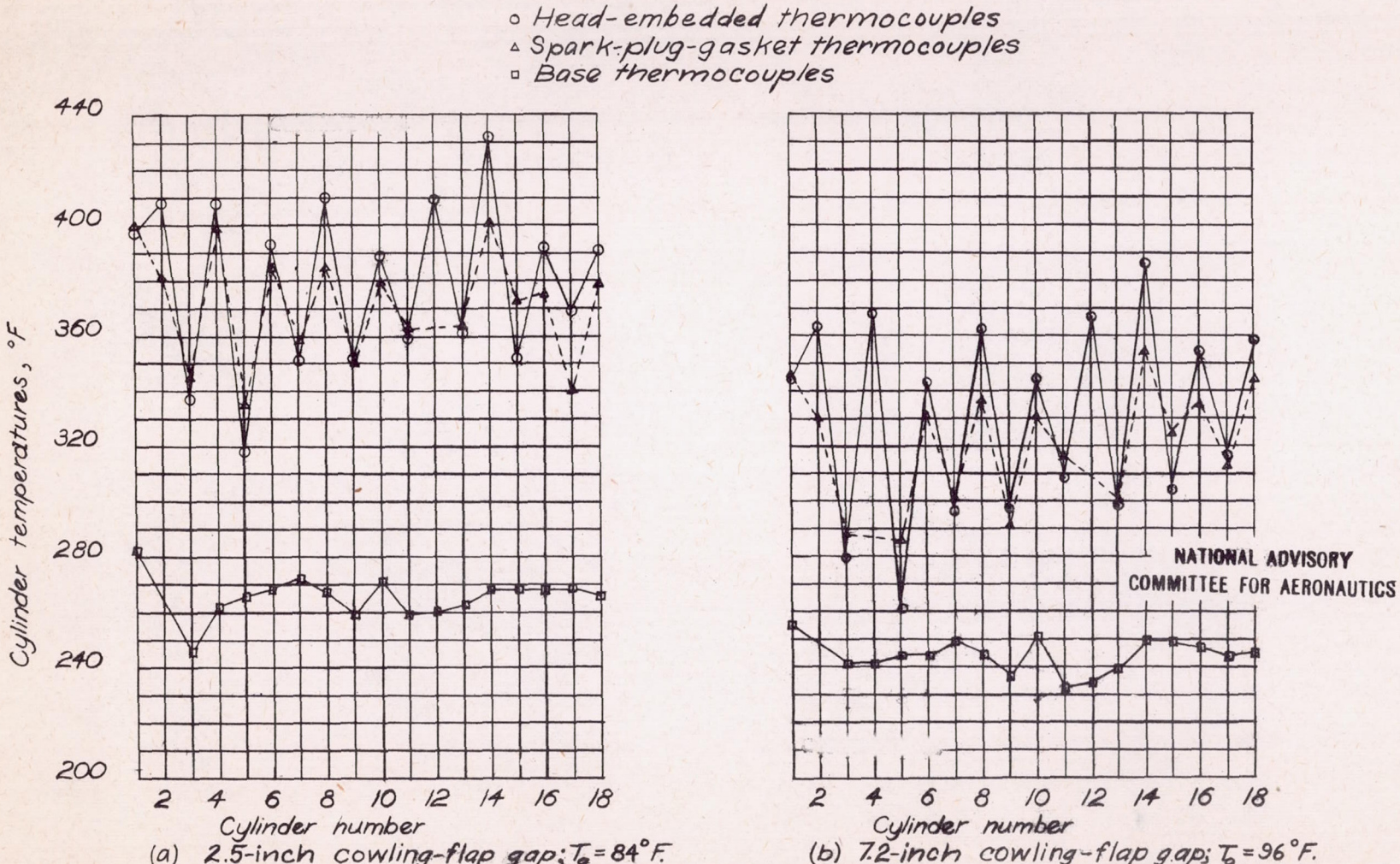

(a) 2.5-inch cowling-flap gap; T_a = 84° F. (b) 7.2-inch cowling-flap gap; T_a = 96° F.

Figure 29. – Typical temperature pattern 1100 bhp; 2120 rpm; fuel-air ratio, 0.08; V, 260 mph, α_T = 0°.

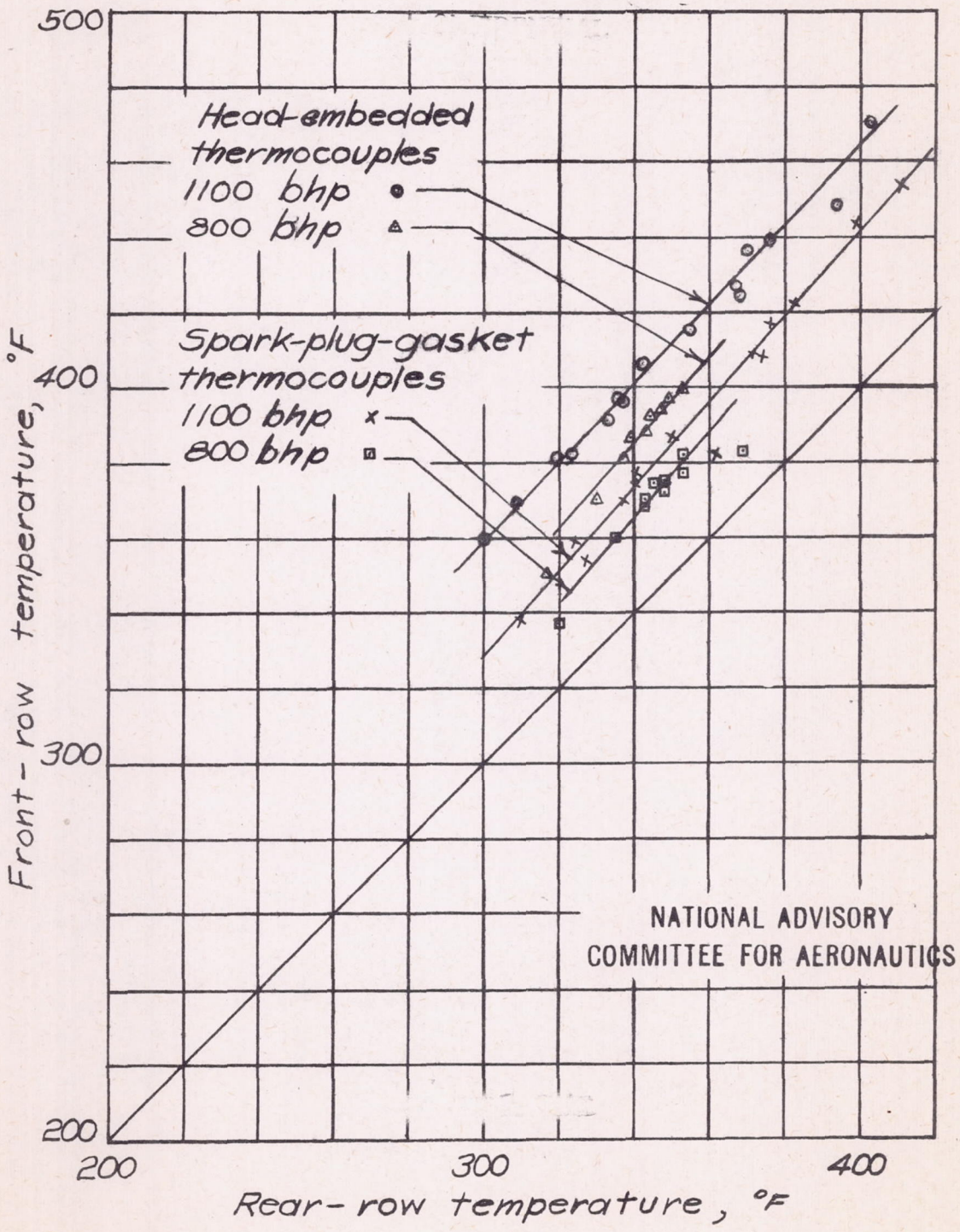

Figure 30.— Comparison of average temperature of front cylinders with average of rear cylinders. Fuel-air ratio, 0.08.

$$\text{Define: } ihp = bhp + \left[27 + 2.4\left(\frac{We}{1000}\right)\right]\left(\frac{N}{1000}\right)^2 - 1.735\left(p_{e_{SL}} - p_{e_{alt}}\right)\left(\frac{N}{1000}\right)$$

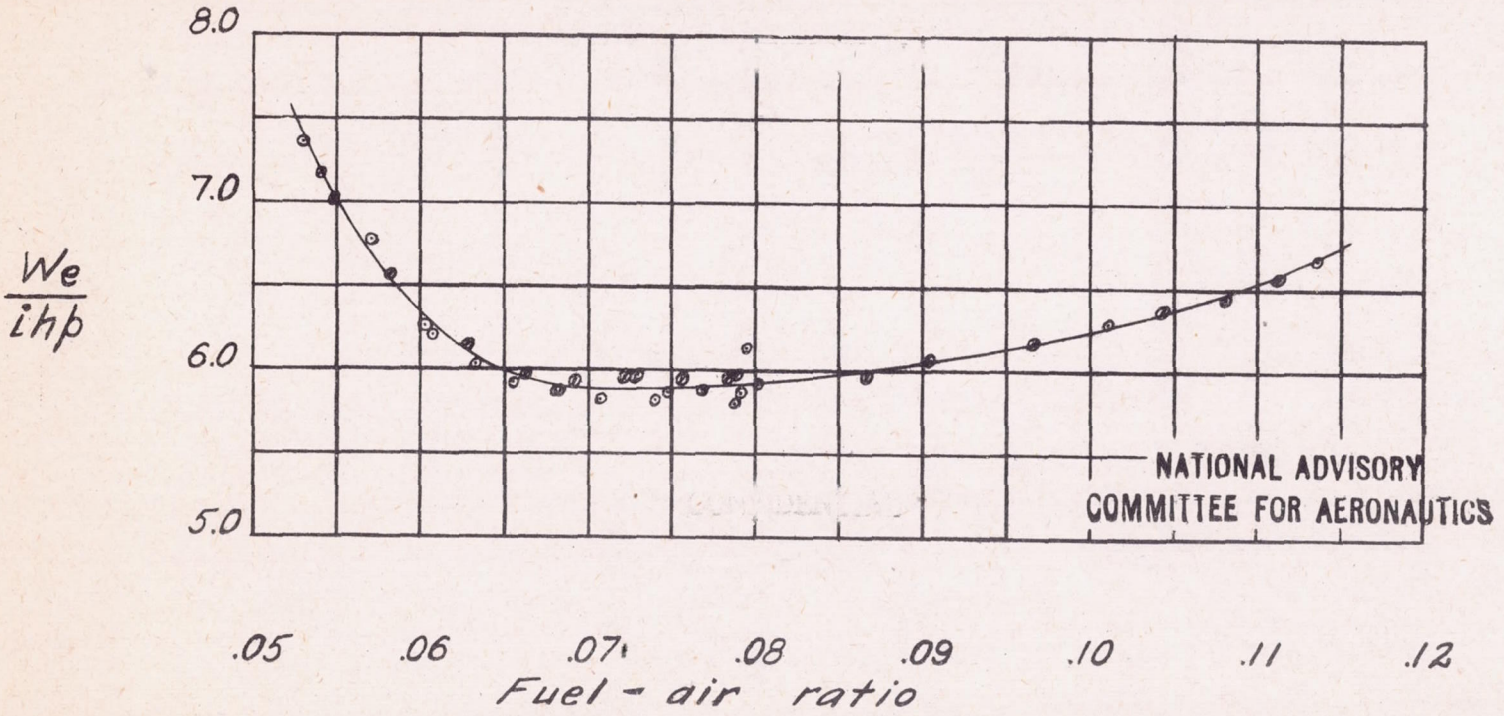

Figure 31. - Variation of indicated specific air consumption with fuel-air ratio. P. & W. R-2800 engine, B-series.

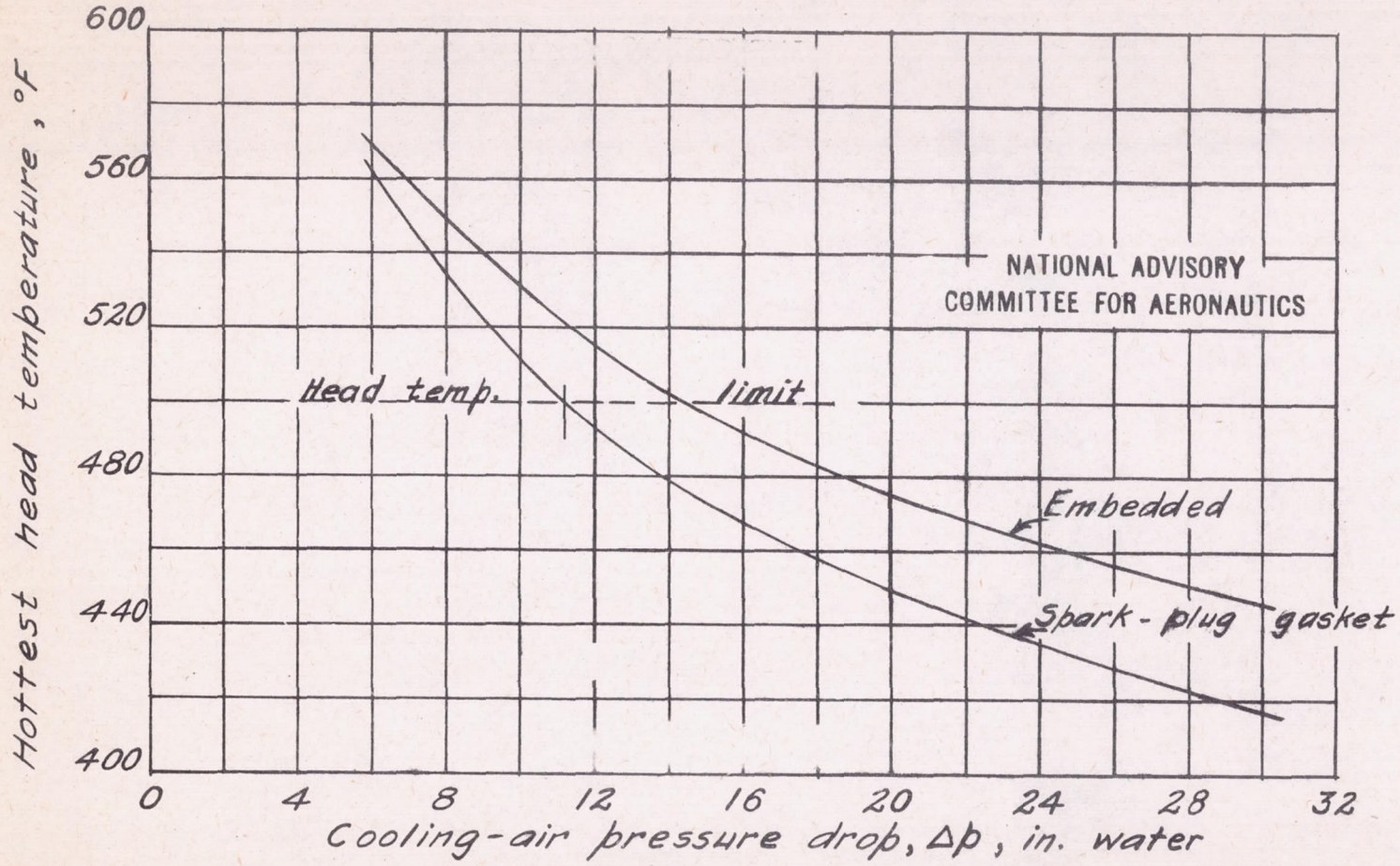

Figure 32.- Variation of hottest head temperatures with cooling-air pressure drop. P & W. R-2800 engine, B-series; 2000 bhp; 2700 rpm; fuel-air ratio, 0.107; sea-level Army summer air. Calculated from the engine-cooling correlation.

3-15-43 B.W.C.